Arizpe sub-basin: A sedimentary and volcanic record of Basin and Range extension in north-central Sonora, Mexico

Carlos M. González-León[1,*], Víctor A. Valencia[2], Margarita López-Martínez[3], Hervé Bellon[4], Martín Valencia-Moreno[1], and Thierry Calmus[1]

[1] *Estación Regional del Noroeste, Instituto de Geología, Universidad Nacional Autónoma de México, ApartadoPostal 1039, 83000 Hermosillo, Sonora, Mexico.*
[2] *Geosciences Department, University of Arizona, Tucson, Arizona 85721, USA.*
[3] *Departamento de Geología, Centro de Investigación Científica y de Educación Superior de Ensenada (CICESE), Km 107 Carretera Ensenada-Tijuana No. 3918, 22860 Ensenada, Baja California, Mexico.*
[4] *UMR 6538, Domaines Océaniques, IUEM, Université de Bretagne Occidentale, 6, Av. Le Gorgeu, Brest, 29285, France.*
* cmgleon@unam.mx

ABSTRACT

The Arizpe sub-basin located in the northern part of the Río Sonora basin is a Basin and Range half-graben that initiated during Late Oligocene time in north-central Sonora. Its ~2.1 km-thick, east-dipping volcanic and sedimentary fill assigned to the Báucarit Formation is divided, from base upwards, into the following informal members. The La Cieneguita member composed of interbedded conglomerate, siltstone and gypsum beds which unconformably overlay older Cenozoic volcanic rocks; the El Toro Muerto basalt composed of basalt flows, basalt breccia and subordinate conglomerate beds; the Arizpe conglomerate composed of three fining-upwards conglomerate sequences that interdigitates with flows of the Tierras Prietas basalt in its lower part and the Agua Caliente basalt in its upper part; the Bamori member is a coarsening-upward succession of siltstone, sandstone and conglomerate that unconformably overlies the Arizpe conglomerate and it is unconformably overlain by the sedimentary El Catalán breccia. Basin accommodation started at ~25 Ma when deposition of the La Cieneguita member, followed by alkaline basaltic volcanism of the El Toro Muerto and contemporaneous rhyolitic volcanism, floored the area predating significant clastic deposition. The Agua Caliente basalt (~21 Ma) in the upper part of the basin fill indicates the basin was rapidly subsiding.

Multiple phases of normal faulting affected the Arizpe sub-basin. The main controlling structure may be the steep (80°), west-dipping, sub-parallel El Fuste and Granaditas normal faults that bound the Arizpe sub-basin at its present-day eastern margin, or there may be a fault or faults that were subsequently buried beneath younger basin fill near the eastern margin of the basin. The basin was disorganized by an even younger NW-SE phase of normal faulting represented by the southwest-dipping Crisanto and Tahuichopa faults. Growth strata within basin fill suggests that syntectonic deposition was active during all phases of normal faulting. However, punctuated tectonic activity on these faults may have controlled deposition of conglomerate sequences of the Arizpe conglomerate.

Geochemical data from the El Toro Muerto, the Tierras Prietas and the Agua Caliente basalt members indicate they are high-K, alkaline to subalkaline basaltic trachyandesites with light REE-enriched patterns, initial Sr ratios between 0.7069 and 0.7076, and εNd values between -3.76 and -4.88. Pb isotopic values from two samples of the El Toro Muerto basalt yielded very similar results, and along

---

with the other geochemical data suggest an important participation of the continental lithosphere as magma source for this volcanism.

　　The data herein reported are supported by eight new geochronologic ages and they contribute to better document and constrain the timing of magmatism and extension in the Basin and Range tectonic province in Sonora.

Key words: magmatism, geochronology, Oligocene, Miocene, Basin and Range, Sonora, Mexico.

RESUMEN

　　La subcuenca de Arizpe, localizada en la parte norte de la cuenca del Río Sonora, es un medio graben que empezó a formarse durante el Oligoceno Tardío asociado a la deformación de Sierras y Valles Paralelos (Basin and Range). Su relleno volcánico y sedimentario de ~2.1 km de espesor, el cual buza hacia el oriente, se asigna a la Formación Báucarit y se divide, de la base a la cima, en los siguientes miembros informales. El miembro La Cieneguita, formado por conglomerado con intercalaciones de limolita y yeso, que sobreyace discordantemente a rocas volcánicas cenozoicas más antiguas; el basalto El Toro Muerto, formado por derrames de basalto, brecha basáltica y en menor proporción por conglomerado. El conglomerado Arizpe, formado por tres secuencias conglomeráticas grano decreciente hacia su cima y con interdigitaciones del basalto Tierras Prietas en su parte inferior y del basalto Agua Caliente en su parte superior. El miembro Bamori, formado por limolita, arenisca y conglomerado en secuencia grano-creciente hacia su cima, sobreyace en discordancia al conglomerado Arizpe y está a su vez sobreyacido discordantemente por la brecha El Catalán formada por clastos de basalto. La subcuenca Arizpe empezó a formarse hace ~25 Ma cuando la sedimentación terrígena del miembro La Cieneguita y el volcanismo alcalino del basalto El Toro Muerto precedieron a la sedimentación clástica del conglomerado Arizpe. La edad de ~21 Ma obtenida del basalto Agua Caliente, que ocurre en la parte superior del relleno de la cuenca, indica que ésta fue una cuenca de subsidencia rápida.

　　El fallamiento normal que inició a la cuenca tuvo lugar cerca de su actual margen oriental y controló el depósito de las secuencias conglomeráticas. En esa posición se ubican las fallas normales El Fuste y Granaditas que buzan al poniente, pero es probable que la falla principal se encuentre actualmente cubierta debajo de rocas más jóvenes del relleno de la cuenca. El fallamiento sinsedimentario fue importante y, después de su formación, la sub-cuenca Arizpe fue desorganizada por fallamiento normal de rumbo NW-SE representado por las fallas Crisanto y Tahuichopa.

　　Datos geoquímicos de los basaltos El Toro Muerto, Tierras Prietas y Agua Caliente indican que corresponden a traquiandesitas basálticas ricas en K, que varían de alcalinas a subalcalinas con un patrón de enriquecimiento en tierras raras ligeras, con relaciones isotópicas de Sr inicial entre 0.7069 y 0.7076 y valores iniciales de εNd entre -3.76 y -4.88. Análisis isotópicos de Pb en dos muestras del basalto El Toro Muerto arrojan valores muy parecidos y, en conjunto, estos datos sugieren una participación importante de la litósfera continental como fuente de los magmas de este volcanismo.

　　Los datos reportados se apoyan además en ocho nuevos fechamientos y contribuyen a documentar el tiempo del magmatismo y la extensión de la provincia tectónica de la Basin and Range en Sonora.

Palabras clave: magmatismo, tectónica, geocronología, Oligoceno, Mioceno, Basin and Range, Sonora, México.

INTRODUCTION

　　Although most of the state of Sonora is located within the late Cenozoic southern Basin and Range extensional province and the sedimentary and volcanic fill of numerous NNW-SSE-oriented basins that formed during this tectonic event are well exposed, only a few studies have been conducted to understand their sedimentary, magmatic and tectonic history. King (1939) first noted that the fills of these valleys in southern Sonora are mostly composed of a lower basaltic member and an upper conglomerate member that he named as the Báucarit Formation in outcrops at the town of Báucarit (Figure 1).

　　Other workers suggested that not all of the late Cenozoic extensional basins in Sonora share similar sedimentary and magmatic histories (Gans, 1997; McDowell *et al*., 1997) and applied different informal names to their fill deposits. The first attempts to understand the sedimentary history of some of these basins were conducted by Miranda-Gasca and DeJong (1992) and De la O-Villanueva (1993), who studied the Magdalena and the Río Yaqui basins (Figure 1), respectively. Other authors studied the Ures basin in central Sonora (Calles-Montijo, 1999; Vega-Granillo and Calmus, 2003). McDowell *et al*. (1997) and Gans (1997), however, studied in more detail the magmatism and tectonic development of the late Cenozoic basins
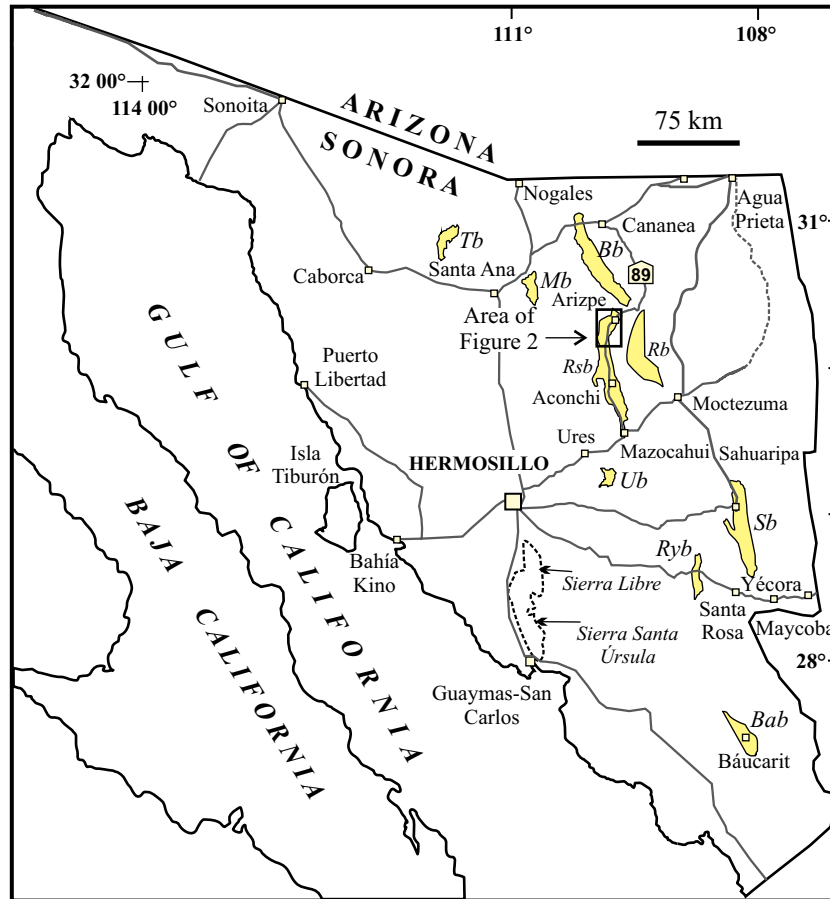
Figure 1. Location map of the Río Sonora basin, and other Basin and Range Sonoran basins, and localities mentioned in this work. Tb, Tubutama basin; Mb, Magdalena basin; Bb, Bacanuchi basin; Rsb, Río Sonora basin; Ub, Ures basin; Sb, Sahuaripa basin; Ryb, Río Yaqui basin; Rb, El Rodeo basin; Bab, Báucarit basin. Black rectangle indicates the location of the Arizpe sub-basin and of geologic map of Figure 2; area enclosed by dashed line indicates the location of Sierra Santa Úrsula and Sierra Libre.

in the Río Yaqui region and nearby areas of south central Sonora. Their results indicate that the fills of the Basin and Range basins are dominated by mafic flows in their lower parts and by conglomerate in their upper parts, and in most cases the name Báucarit Formation was applied to describe that succession.

The Río Sonora basin is an informal name that we apply to one of these N-S-elongated Basin and Range grabens located in the north-central part of Sonora, between the towns of Arizpe and Mazocahui (Figure 1). This basin is 100 km-long and 15 to 25 km-wide. Our results indicate that the Río Sonora basin is a tectonically and sedimentologically complex half-graben that is limited to the east and west by elevated mountains ranges composed of sedimentary, volcanic and plutonic rocks, which range in age from Proterozoic to Miocene. At its northern and southern boundaries, the Río Sonora basin is in fault contact with high mountainous ranges.

In this work, we present results for the northernmost part of the Río Sonora basin located near the town of Arizpe, which we name the Arizpe sub-basin. The well-exposed sedimentary and volcanic fill of this sub-basin allows for its stratigraphic and structural relationships to be easily studied. Our aim is to contribute to the understanding of the sedimentary and magmatic history of a typical, complexly-deformed graben located within the Basin and Range province of Sonora based on geologic mapping, detailed measurement of the entire basin stratigraphic section, and on geochronology, geochemical and radiogenic isotopic analyses of some of the interbedded volcanic flows.

GEOLOGIC SETTING

The Arizpe sub-basin is a N-S- striking half-graben filled by a Late Oligocene-Early Miocene, eastward thickening succession of interbedded mafic flows, subordinate ash-fall tuffs and ignimbrite, and clastic rocks that González-León *et al.* (2000) first assigned to the Arizpe conglomerate. The basin was developed over a basement composed of strata assigned to the Lower Cretaceous Bisbee Group and to Upper Cretaceous - Cenozoic volcanic rocks of the Tarahumara Formation (González-León *et al.*, 2000) (Figure 2). A rhyolitic unit with minor basalt flows that crops out
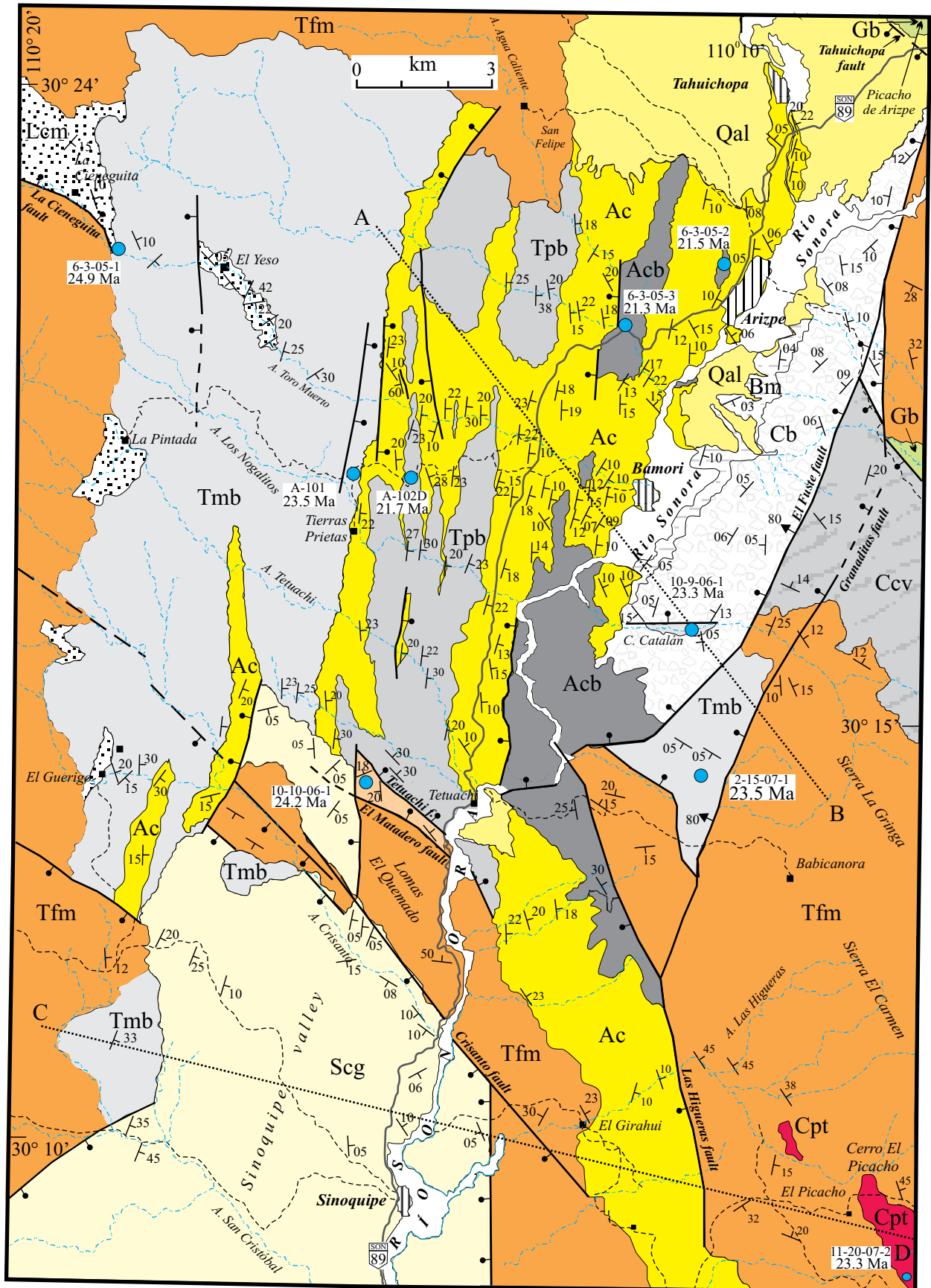
Figure 2. Geologic map of the Arizpe sub-basin in the Río Sonora basin, and accompanying structural sections A-B and C-D.
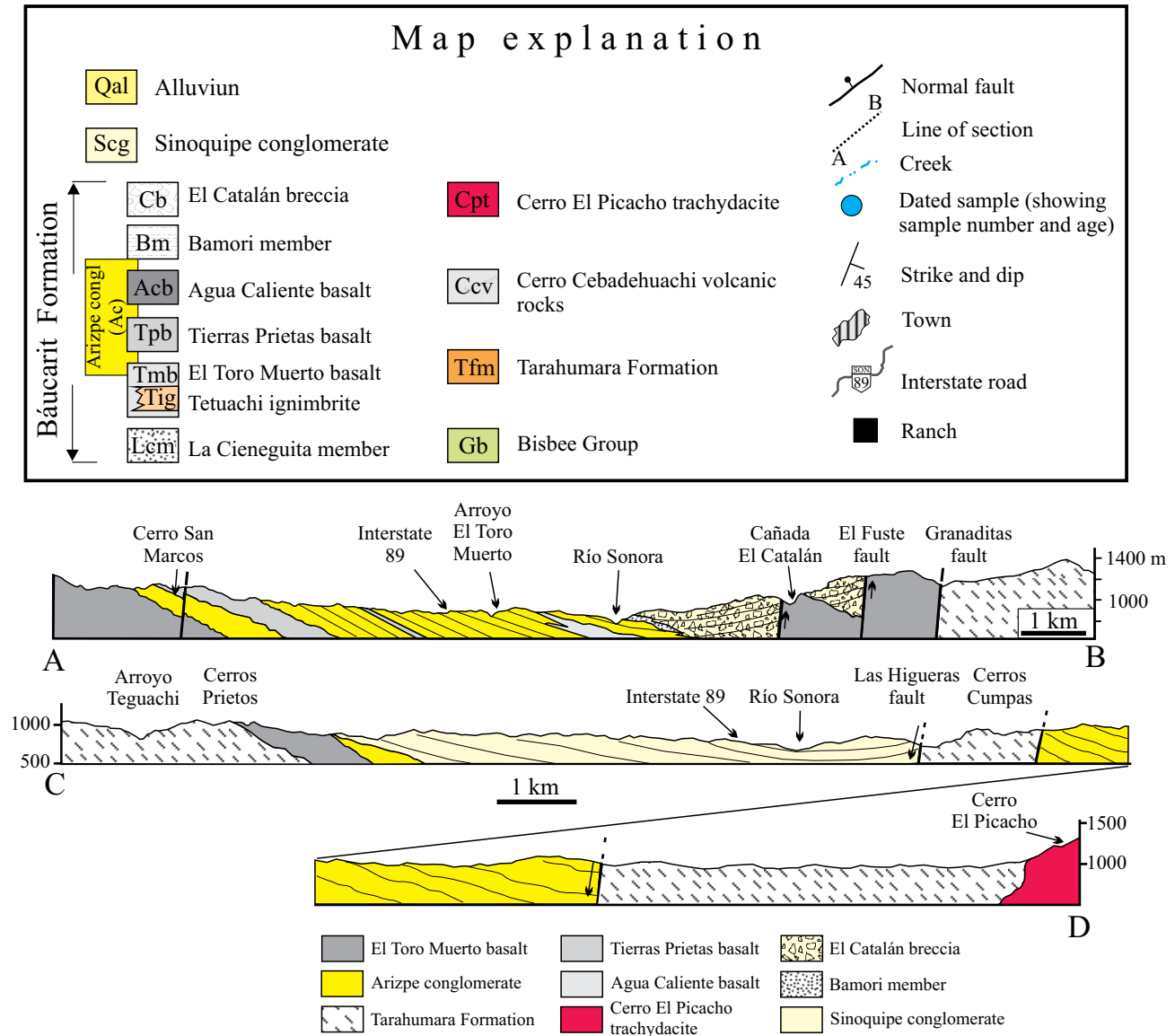
Map explanation

Figure 2 (continued). Geologic map of the Arizpe sub-basin in the Río Sonora basin, and accompanying structural sections A-B and C-D.

in the eastern part of the area might be correlative with the Cerro Cebadehuachi volcanic rocks, a unit of Oligocene age that was reported from its outcrops about 10 km north of the study area (González-León *et al.*, 2000). Based on our more detailed stratigraphic study, we divide the basin-fill succession into seven members, restrict the term Arizpe conglomerate to one of them and reassign the whole succession to the Báucarit Formation.

From base upwards, the Báucarit Formation is composed of the following informal members: La Cieneguita member, El Toro Muerto basalt, the Arizpe conglomerate that laterally interfingers with the Tierras Prietas and Agua Caliente basalt members, the Bamori member and the El Catalán breccia (Figures 2 and 3).

The Báucarit Formation is exposed in the Arizpe valley but in this study the continuous stratigraphic thickness of the La Cieneguita member, El Toro Muerto basalt and the Arizpe conglomerate were measured with a Jacob's staff along the El Toro Muerto creek, between rancho La Cieneguita to the west and the town of Bamori to the east (Figure 2). The uppermost part of the Arizpe conglomerate was measured along Interstate road 89 from the Arroyo Agua Caliente to the town of Tahuichopa (Figure 2). Along the El Toro Muerto section the Arizpe conglomerate interdigitates in its lower part with the Tierras Prietas basalt, and in its upper part with the Agua Caliente basalt members (Figure 3). The thickness of the Tierras Prietas and Agua Caliente basalts were estimated from their more complete outcrops along the arroyo Tetuachi creek located about 6 km south of the El Toro Muerto Creek and along the gorge cut by the Río Sonora just south of the town of Bamori, respectively (Figure 2). The thickness of the Bamori member was mea-
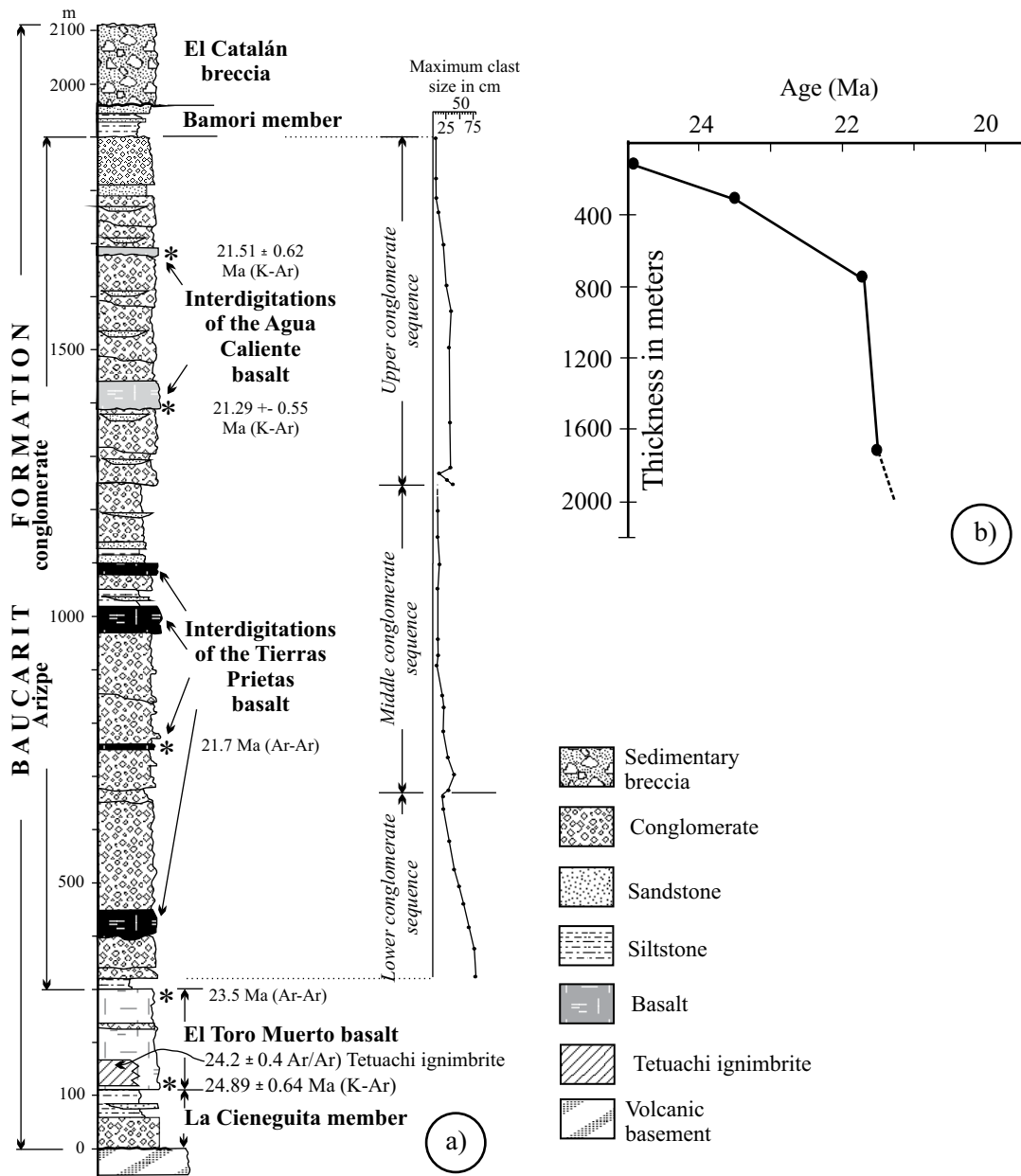
Figure 3. a) Stratigraphic column of the Báucarit Formation in the Arizpe sub-basin showing the position of dated samples. The plot to the right shows the size in cm of the largest measured clasts, and defines three fining-upward sequences in the Arizpe conglomerate. b) Non-decompacted subsidence curve of the Báucarit Formation in the Arizpe sub-basin.

sured in outcrops located just east of the town of Bamori, and the thickness of the Catalán breccias was estimated from outcrops along the Cañada Catalán located southeast of the town of Bamori. A 1:50,000-scale geologic mapping of the study area was refined from previous works by González-León *et al*. (2000) and González-Gallegos *et al*. (2003). To constrain the age of the Báucarit Formation we report four new Ar-Ar ages, three K-Ar ages and one U-Pb zircon age of mafic and rhyolite rocks. These data are complemented with two Ar-Ar ages reported by González-León *et al*. (2000) from the study area, as discussed below. Additionally, we include seven new geochemical analyses and three Sr-Nd-Pb

isotopic analyses of volcanic rocks which are complemented with previous geochemical data reported in González-León *et al*. (2000).

STRATIGRAPHY

The *La Cieneguita member* (Figures 2 and 3) consists in its lower part of a 60 m-thick package of pebble conglomerate and coarse-grained sandstone that stratigraphically grades upwards into a 50 m-thick interval of reddish brown mudstone-siltstone, with interbedded gypsum (beds

< 5 cm thick) and granule to fine-grained sandstone (thin to medium beds). This member unconformably rests on altered volcanic rocks assigned to the Tarahumara Formation or on rhyolitic tuffs of probable Oligocene age (not differentiated in Figure 2). The La Cieneguita member is not always present at the base of the Arizpe Conglomerate, probably because it was partly eroded after deposition or because it was deposited on an uneven erosional surface, and where this occurs, the El Toro Muerto basalt unconformably rests on the older rocks.

The *El Toro Muerto basalt* sharply overlies the La Cieneguita member, and consists of basalt flows, basalt breccia and subordinate conglomerate beds (Figures 2 and 3). The basalt flows are fine-grained and petrographically classify as porphyritic olivine basalt with phenocrysts of plagioclase and scarce augite pyroxene in a pseudotraquitic matrix of microlitic andesine (An $_{34\text{-}50}$). A local, 100 m-thick outcrop of a rhyolitic welded tuff exposed through a fault contact in the central part of the area and that we informally name the Tetuachi ignimbrite, is a probable interdigitation of the Tierras Prietas basalt, according to its geochronologic age (Figure 3). The El Toro Muerto basalt is in turn stratigraphically overlain by the Arizpe conglomerate, but toward the southwestern part of the study area these members are interbedded (Figure 2). The estimated thickness of this member is 200 m.

The stratigraphic column of the *Arizpe conglomerate* is 1,600 m-thick along the measured section of the El Toro Muerto creek. The lowermost part of the El Toro Muerto conglomerate consists of a 20 m-thick interval of massive, green to light gray siltstone, whereas the remainder upper part of the succession is predominantly conglomerate that forms three fining-upward sequences distinguished on the basis of their maximum clast sizes. These sequences are described below as the lower, middle and upper conglomerate sequences (Figure 3).

The lower conglomerate sequence is 340 m thick (Figure 3) and in its lower part consists of poorly-sorted, pebble to cobble conglomerate with clasts (mostly <10 cm long) of basalt (~60%), andesite (~20%), rhyolite (~15%) and scarce diorite (Figure 4a). The largest clasts are scattered cobbles of basalt up to 80 cm-long. A few beds of white, lithic- and crystal-rich ash-fall tuffs up to 3 m thick (Figure 4b) are interbedded within this part of the section, along with a 50 m-thick flow of the Tierras Prietas basalt. The middle and upper parts of this lower sequence mostly consists of poorly sorted, subangular to subrounded pebble-conglomerate in beds up to 3 m thick, but they more commonly occur in beds less than 60 cm thick, because of abundant reactivation surfaces. The conglomerate beds are mostly clast-supported and commonly have interbeds of thin, lenticular, coarse-grained to granule sandstone, which occasionally show fining-upward cycles. Planar cross-stratification and large-scale trough cross-stratification are locally present. In the upper part of this sequence, the largest clasts are of basalt and decrease in size to 20 cm.

The middle conglomerate sequence is 590 m thick and also has interdigitations of the Tierras Prietas basalt. Conglomerate beds in this cycle are up to 3 m thick but abundant reactivation surfaces (multistory) obliterate the original thicknesses of the fining-upward cycles. These beds are mostly pebble and rarely cobble, poorly sorted, subangular conglomerate with local, poorly-developed planar and trough cross-stratification. The largest clasts in this sequence are scattered fragments of basalt that reach up to 40 cm long in the lower part and are up to 6 cm long in its upper part. Near its upper part, the sequence has intervals up to 30 m thick of well stratified and well consolidated fine- to coarse-grained sandstone with interbedded yellow to reddish, bioturbated siltstone and white ash-fall tuffs beds (Figure 4c). The sequence ends with a 110 m thick pebble conglomerate (clasts <5 cm long) with interbeds of thin- to medium-bedded, lenticular, fine- to coarse-grained sandstone. Clast compositions in this sequence are of andesite (~50%), basalt (~35%) and rhyolite (~15%).

The upper conglomerate sequence is 650 m thick and consists of medium to thick, poorly defined beds of pebble conglomerate, sandy pebble conglomerate, pebble sandstone and more rarely cobble conglomerate in beds up to 4 m thick, with lenticular beds of coarse- to medium-grained sandstone. Beds composing fining-upward sequences can be present, but their upper parts are generally cut by abundant reactivation surfaces. The conglomerate is mostly clast-supported, but matrix-supported conglomerate also occur. Clasts are poorly sorted, subrounded to subangular, and consist of andesite (~50%), rhyolite (~40%) and basalt (~10%). Planar and trough cross stratification in bedsets up to 40 cm thick and crude horizontal stratification of clasts occasionally occurs. The largest clasts in the lower part of this sequence are of basalt and reach up to 35 cm in length. The uppermost 150 m of this sequence consists of poorly sorted, clast-supported, subrounded pebble conglomerate, with a rich matrix of pebble to granule sandstone that interbeds with fine- to coarse-grained, lenticular sandstone. These lithologies grade to the top of the sequence to well-stratified granule and coarse-grained sandstone. Reactivation surfaces are abundant in the upper part of the sequence, whereas sandstone beds up to 50 cm thick are more laterally continuous. Maximum clast sizes in this part of the sequence reaches 10 cm in length and consist of andesite (~50%), rhyolite (~30%), dacite (~10%) and basalt (~10%). At its middle and upper parts this sequence has interdigitations of the Agua Caliente basalt.

The *Tierras Prietas basalt* has a thickness of about 700 m estimated from outcrops along the Tetuachi creek, located south of the El Toro Muerto creek (Figure 2). This member consists of superimposed 50 to 100 m-thick, fine-grained flows of basalt and basaltic breccias, which in their upper parts develop reddish, altered intervals up to 20 m thick of probably pedogenic origin (Figure 4d). Petrographically, this rock is a porphyritic olivine basalt with phenocrysts of plagioclase (An $_{38\text{-}50}$) and subordinate clinpyroxene (au-
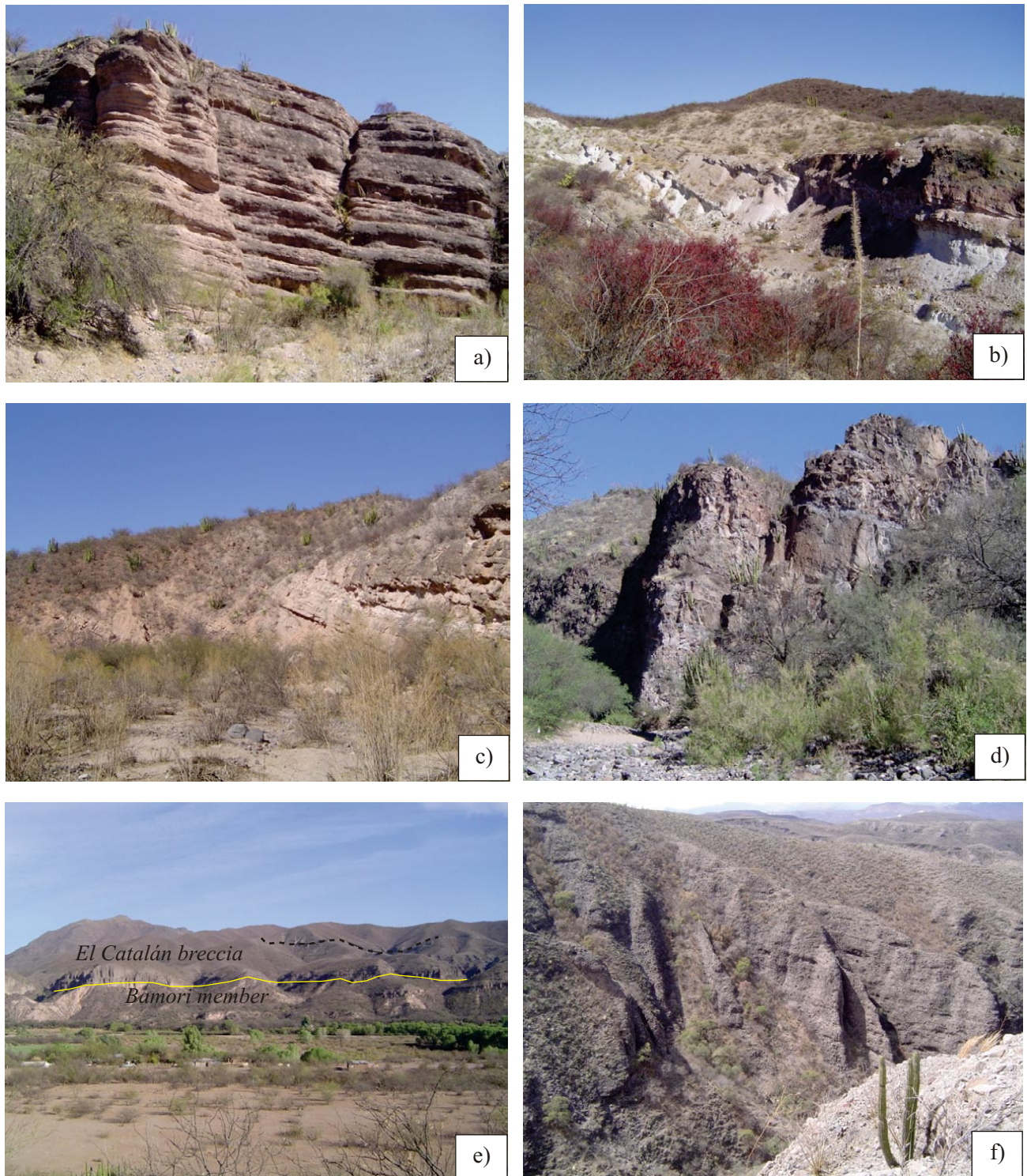
Figure 4. Outcrop photographs of the Báucarit Formation in the Arizpe sub-basin. a) Poorly sorted, pebble to cobble conglomerate of the lower part of the Arizpe conglomerate member, along arroyo El Toro Muerto. Outcrop height about 35 m. b) Lithic- and crystal-rich ash-fall tuffs interbedded in the lower part of the Arizpe conglomerate member. c) Fine- to coarse-grained sandstone and interbedded yellow to reddish, bioturbated siltstone and white ash-fall tuffs beds in the upper part of the middle sequence of the Arizpe conglomerate member. d) Basaltic and basaltic breccia of the Tierras Prietas basalt developing reddish, altered intervals of probably pedogenic origin at their tops. Outcrop at Tetuachi creek. Height of hills in foreground from base of creek is ~60 m. e) Unconformable contact (yellow line) between the Bamori and the El Catalán members in the Río Sonora east of the town of Bamori. El Fuste fault (thick, dashed black line) separates the El Catalán breccia from interbedded rhyolite and basalt of supposed Oligocene age. f) Outcrop of the crudely stratified El Catalán breccia dipping to the west in hills located just east of the town of Bamori (photograph viewing toward the southwest).

Table 1. Summary of geochronologic ages of dated samples from the study area, including data previously reported by González-León *et al*. (2000).

Unit	Sample	UTM Location	Age
Tetuachi ignimbrite	10-10-06-1	12R 571932E; 3345454N	24.2±0.2 Ma (Ar/Ar)
El Toro Muerto basalt (lowermost part)	6-3-05-1	12R 566338E; 3356954N	24.89 ± 0.64 Ma (K/Ar, whole-rock)
El Toro Muerto basalt	10-9-06-1	12R 578845E; 3348784N	23.3±0.3 Ma (Ar/Ar)
El Toro Muerto basalt	2-15-07-1	12R 579239E; 3345637N,	23.5±0.2 Ma (Ar/Ar).
El Toro Muerto (uppermost part)	A-101	12R 571640E; 3352300N	23.52±0.17 Ma (Ar/Ar; González-León *et al*., 2000).
Cerro El Picacho	11-20-07-2	12R 583523E; 3334488N	23.3 ± 0.6 Ma (U/Pb)
Tierras Prietas basalt	A-102D	12R 573903E; 3352512N	21.70±0.20 Ma (Ar/Ar; González-León *et al*., 2000).
Agua Caliente basalt	6-3-05-3	12R 577704E; 3354968N	21.29 ± 0.55 Ma age (K/Ar, whole-rock).
Agua Caliente basalt	6-3-05-2	12R 579372E; 3357108N	21.51 ± 0.6 Ma (K/Ar, whole-rock)
El Pajarito basalt	9-23-08-5	12R 605576E; 3321056N	18.6 ± 0.2 (Ar/Ar)

gite?), sorted in a rich pseudotraquitic matrix of microlitic plagioclase. Along the El Toro Muerto measured section, flows of the Tierras Prietas basalt laterally interdigitate with the lower and middle conglomerate sequences of the Arizpe conglomerate (Figure 3).

The *Agua Caliente basalt* has an estimated thickness of 300 m in outcrops along the Río Sonora gorge, just south of the town of Bamori (Figure 2). The Agua Caliente basalt consists of poorly stratified, fine-grained mafic flows and breccia. The basalt flows display abundant calcite-filled cavities and petrographically show an abundant pseudotraquitic matrix of microlitic plagioclase with scarce phenocrysts of plagioclase (An_{39-53}), olivine and clynopyroxene.

The *Bamori member* is a 60 m-thick clastic interval that unconformably overlies the upper conglomerate sequence in outcrop exposed east of the Río Sonora (Figure 4e). It forms a thin, E-NE strip outcrop with shallow dips to the east. It is a coarsening-upward succession of massive, bioturbated siltstone and fine grained sandstone in its lower part, and massive, fine-grained sandstone with intercalations of medium-bedded, coarse-grained sandstone in cosets up to 5 m thick that show fining-upward successions in its middle part. The uppermost 20 m of this member consists of granule sandstone and lenticular, medium-bedded pebble conglomerate that are the lags of large-scale, epsilon cross-stratification.

The *El Catalán breccia* has an estimated thickness of 150 m and crops out in the eastern margin of the Arizpe basin. It is a coarse, crudely stratified breccia with clasts up to 2 m long (Figure 4f). The clasts are angular and poorly sorted, and most beds are matrix-supported. The matrix is a mixture of coarse sand and granules with occasional thin to medium, lenticular beds of granule conglomerate. The clasts are mostly derived from basalt (90%), but there are also clasts of andesite and rhyolite. This member shallowly dips to the west and unconformably overlies the Bamori member which dips to the east.

GEOCHRONOLOGY

A sample from the lowermost part of the El Toro Muerto basalt yielded a K-Ar age at 24.89 ± 0.64 Ma (sample 6-3-05-1; Tables 1 and 2, Figure 2), similar (within error) to an Ar-Ar (plateau age), sanidine age of 24.2 ± 0.4 Ma obtained from the Tetuachi ignimbrite (sample 10-10-

Table 2. K-Ar age data for three samples of the Báucarit Formation in the study area.

Sample code	Location	Lab.Ref.	1 Mean age (Ma)	2 Age (Ma)	±	error (1 σ)	4	5 K_2O (wt. %)	6 $^{40}Ar_R$ (10^{-7} cm³ g⁻¹)	7 $^{40}Ar_R$ (%)	8 Molten weight (g)
6-3 -05-2	Agua Caliente	B 7204-1	21.51	21.31	±	0.63		2.48	17.41	55.7	0.9871
		B 6916-4		21.73	±	0.61		2.48	17.49	70.9	0.8090
6-3-05-3	Agua Caliente	B 6944-4		21.29	±	0.55		2.86	19.75	73.5	0.8195
6-3-05-1	El Torro Muerto	B 6921-9		24.89	±	0.64		1.99	16.08	79.1	0.8342

Column 1: Laboratory reference; B means Brest laboratory, 7204 is the chronological order of this experiment in the whole range of argon extractions done in the laboratory; -1 is the order of this extraction in a full series of experiments, *i.e.*, 9 to 10 samples using the same molybdenum crucible, including at least one standard sample of glauconite GLO, for an overall calibration and control test. Column 2: The mean age results from two independent age determinations, *i.e.*, for two different argon extractions from rock grains under vacuum and their further isotopic analyses by mass spectrometry. Columns 3 and 4 : Ages are calculated with the constants recommended by Steiger and Jäger (1977) and errors are quoted at one sigma level after the calculations by Mahood and Drake (1982). Column 5: K contents were measured by atomic absorption spectrometry after a chemical attack at 80°C of a representative powder sample rock using hydrofluorhydric acid.
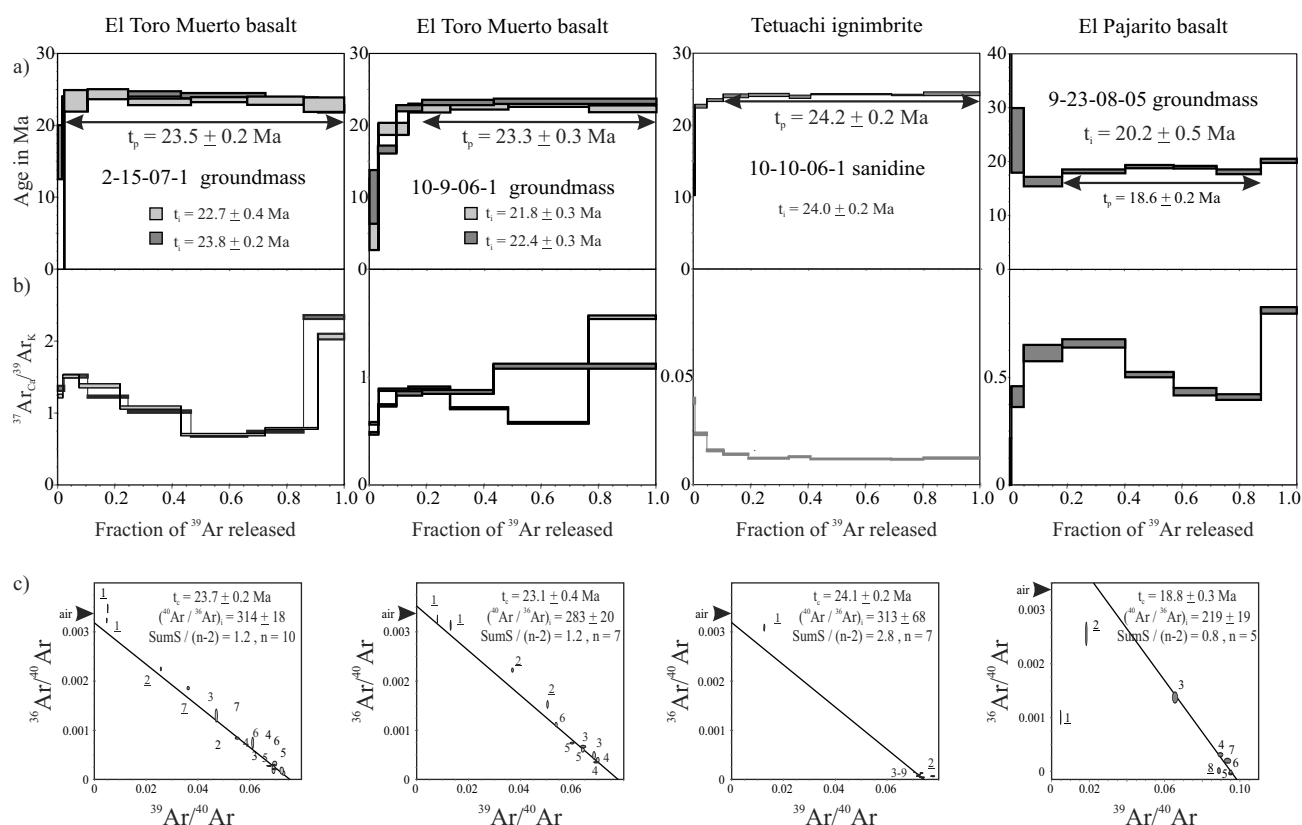
Figure 5. $^{40}Ar/^{39}Ar$ results. Samples 2-15-07-1 and 10-9-06-1 of the El Toro Muerto basalt, and 10-10-06-1 of the Tetuachi ignimbrite are from the study area. Sample 9-23-08-5 is from the El Pajarito basalt in the El Rodeo basin. For each sample: a) age spectrum; b) $^{37}Ar_{Ca}/^{39}Ar_k$ diagram; c) $^{36}Ar/^{40}Ar$ versus $^{39}Ar/^{40}Ar$ correlation diagram.

06-1; Figure 5, Tables 1 and 3, Appendix). We also dated two basaltic samples from outcrops in the southeastern part of the area, which yielded similar Ar-Ar (plateau) ages at 23.3 ± 0.3 and 23.5 ± 0.2 Ma (samples 10-9-06-1 and 2-15-07-1; Figure 5; Tables 1 and 3). These basalt flows underlie, and are in fault contact with the El Catalán breccia and the Agua Caliente basalt (Figure 2) and we interpret them to belong to the upper part of the El Toro Muerto basalt on the basis of a similar age of 23.52 ± 0.17 Ma (Ar-Ar, sample A-101, Table 1, Figure 3) previously reported by González-León *et al.* (2000) from outcrops of that unit in the central part of the study area. González-León *et al.* (2000) also reported a 21.70 ± 0.20 Ma Ar-Ar age for a basalt flow from the middle part of the Tierras Prietas basalt (sample A-102D, Table 1, Figure 3). In this study, we obtained two K-Ar ages from two samples of the Agua Caliente basalt. The stratigraphically lowermost of these samples yielded an age of 21.29 ± 0.55 Ma age (samples 6-3-05-3, Tables 1 and 2), while the stratigraphically uppermost one yielded an age of 21.51± 0.6 (sample 6-3-05-2, Tables 1 and 2) (Figure 3).

Furthermore, we herein report a U-Pb zircon age of 23.3 ± 0.6 Ma (sample 11-20-07-2, Tables 1 and 4, Figure 6) obtained from a sample of a rhyolite dome exposed at Cerro El Picacho, located at 11 km east of the town of Sinoquipe (Figure 2), which is contemporaneous with the

El Toro Muerto basalt and could represent the source for the Tetuachi ignimbrite. Also, we report a 18.6 ± 0.2 Ma Ar-Ar, plateau age (sample 9-23-08-5, Tables 1 and 3, Figure 5) for a mafic flow informally named the El Pajarito basalt, which is interbedded in the upper part of the conglomeratic basin fill of the El Rodeo basin located east of the Arizpe sub-basin (Figure 1); these data help to constrain younger age of Basin and Range development in this region.

GEOCHEMISTRY AND ISOTOPIC RESULTS

In an effort to characterize the origin and nature of the source of the magmas of the study area, three samples from the El Toro Muerto basalt and one sample from the Agua Caliente basalt were analyzed for major and trace elements and Sr-Nd-Pb isotopic compositions (Tables 5 and 6; analytical procedures are described in the Appendix). We also analyzed major and trace elements from one sample of the Cerro El Picacho dome, one sample from the El Pajarito basalt and another one from the El Huarache basalt (Table 5); this last mafic flows comes from the basal part of the El Rodeo basin fill and we tentatively assume it to be equivalent in age to the El Toro Muerto basalt. The mafic samples from the Arizpe sub-basin plot mostly as alkaline

Table 3. Summary of Ar/Ar data of samples from the study area.

El Toro Muerto basalt 2-15-07-1 groundmass *1st* experiment

pwr	F ^{39}Ar	^{40}Ar*/^{39}Ar$_K$	Age in Ma		% ^{40}Ar*	^{40}Ar/^{36}Ar	^{37}Ar$_{Ca}$/^{39}Ar$_K$	t$_i$ in Ma	t$_p$ in Ma	t$_c$ in Ma	(^{40}Ar/^{36}Ar)$_i$	SumS/(n-2) / n
0.25	0.0229	-1.78 ± 1.64	- 9.8 ± 9.0	†	-2.82	287.40	1.34					
0.50	0.0824	4.29 ± 0.28	23.4 ± 1.5	§	61.58	769.05	1.51					
0.80	0.1403	4.45 ± 0.13	24.3 ± 0.7	§	94.01	4935.11	1.23					
1.10	0.2194	4.26 ± 0.08	23.3 ± 0.5	§	90.49	3107.49	1.02					
1.50	0.1966	4.32 ± 0.07	23.6 ± 0.4	§	96.18	7737.04	0.68					
2.10	0.1970	4.29 ± 0.11	23.4 ± 0.6	§	94.67	5539.12	0.74					
6.00	0.1413	4.19 ± 0.19	22.9 ± 1.0	§	78.02	1344.67	2.34	22.7 ± 0.4	23.5 ± 0.2			

El Toro Muerto basalt 2-15-07-1 groundmass *2nd* experiment

pwr	F ^{39}Ar	^{40}Ar*/^{39}Ar$_K$	Age in Ma		% ^{40}Ar*	^{40}Ar/^{36}Ar	^{37}Ar$_{Ca}$/^{39}Ar$_K$	t$_i$ in Ma	t$_p$ in Ma	t$_c$ in Ma	(^{40}Ar/^{36}Ar)$_i$	SumS/(n-2) / n
0.26	0.0174	2.98 ± 0.69	16.3 ± 3.8	†	4.38	309.04	1.24					
0.50	0.0583	4.28 ± 0.12	23.4 ± 0.7	†	33.56	444.78	1.51					
0.80	0.1430	4.47 ± 0.07	24.4 ± 0.4	§	75.17	1189.89	1.38					
1.10	0.2123	4.46 ± 0.07	24.4 ± 0.4	§	91.86	3628.75	1.08					
1.50	0.2939	4.42 ± 0.07	24.2 ± 0.4	§	93.81	4773.23	0.70					
2.10	0.1839	4.32 ± 0.05	23.6 ± 0.3	§	91.37	3424.58	0.79					
6.00	0.0912	4.08 ± 0.09	22.3 ± 0.5	†	45.11	538.32	2.06	23.8 ± 0.2	24.0 ± 0.2	**23.7 ± 0.2** ‡	314 ± 18	1.2 / 10

El Toro Muerto basalt 10-9-06-1 groundmass *1st* experiment

pwr	F ^{39}Ar	^{40}Ar*/^{39}Ar$_K$	Age in Ma		% ^{40}Ar*	^{40}Ar/^{36}Ar	^{37}Ar$_{Ca}$/^{39}Ar$_K$	t$_i$ in Ma	t$_p$ in Ma	t$_c$ in Ma	(^{40}Ar/^{36}Ar)$_i$	SumS/(n-2) / n
0.30	0.0331	1.39 ± 0.90	7.6 ± 5.0	†	3.40	305.90	0.57					
0.60	0.1035	3.57 ± 0.16	19.5 ± 0.8	†	54.92	655.52	0.88					
0.95	0.1458	4.10 ± 0.11	22.4 ± 0.6	§	85.57	2047.12	0.90					
1.35	0.2022	4.14 ± 0.08	22.6 ± 0.4	§	88.25	2514.10	0.71					
1.90	0.2807	4.21 ± 0.08	23.0 ± 0.4	§	82.29	1668.51	0.58					
6.00	0.2347	4.08 ± 0.09	22.3 ± 0.5	§	67.02	895.92	1.56	21.8 ± 0.3	**22.6 ± 0.2**			

El Toro Muerto basalt 10-9-06-1 groundmass *2nd* experiment

pwr	F ^{39}Ar	^{40}Ar*/^{39}Ar$_K$	Age in Ma		% ^{40}Ar*	^{40}Ar/^{36}Ar^{37}Ar$_{Ca}$/^{39}Ar$_K$		t$_i$ in Ma	t$_p$ in Ma	t$_c$ in Ma	(^{40}Ar/^{36}Ar)$_i$	SumS/(n-2) / n
0.30	0.0310	1.83 ± 0.68	10.0 ± 3.7	†	7.32	318.85	0.48					
0.60	0.0634	3.04 ± 0.10	16.6 ± 0.6	†	34.29	449.68	0.74					
0.95	0.0896	4.10 ± 0.08	22.4 ± 0.4		80.25	1496.25	0.85					
1.40	0.2501	4.24 ± 0.07	23.2 ± 0.4	§	89.69	2867.14	0.86					
6.00	0.5659	4.27 ± 0.07	23.4 ± 0.4	§	78.14	1351.84	1.10	22.4 ± 0.3	23.3 ± 0.3	23.1 ± 0.4 ‡	283 ± 20	1.2 / 7

Continues →

basaltic trachyandesite in the total alkalies versus silica (TAS) diagram (Le Bas *et al*., 1986), similar to previous results obtained from three samples of the Tierras Prietas basalt (samples A-160, A-161 of González-León *et al*., 2000) (Figure 7). The El Huarache and the El Pajarito mafic flows classify as trachybasalt and alkaline trachyandesite, respectively, and the Cerro El Picacho dome is a subalkaline trachydacite (Figure 7). The REE-chondrite-normalized-patterns are very consistent for all these samples, showing an enrichment in the light REE, similar to data reported for the Tierras Prietas basalt by González-León *et al*. (2000) (Figure 8a), but the Cerro El Picacho displays a negative Eu anomaly (Figure 8a). The ^{87}Sr/^{86}Sr isotopic ratios of the El Toro Muerto and Agua Caliente basalts show initial values

between 0.7069 and 0.7076, coupled with negative εNd values between -3.8 and -4.9 (Figure 8b). The Pb isotopic values for the two samples of the El Toro Muerto basalt show consistent ^{208}Pb/^{204}Pb ratios between 38.7 and 39, ^{207}Pb/^{204}Pb ratios near 15.7, and ^{206}Pb/^{204}Pb ratios between 18.7 and 19 (Figure 8c).

SEDIMENTARY AND STRUCTURAL BASIN DEVELOPMENT

On the basis of its regional location and age, and as indicated by its sedimentary, magmatic and structural record (discussed below), the Arizpe sub-basin is a typical half gra-

Table 3 (continued). Summary of Ar/Ar data of samples from the study area.

Tetuachi ignimbrite 10-10-06-1 sanidine

pwr	F ^{39}Ar	^{40}Ar*/^{39}Ar$_K$	Age in Ma		% ^{40}Ar*	^{40}Ar/^{36}Ar^{37}Ar$_{Ca}$/^{39}Ar$_K$		t$_i$ in Ma	t$_p$ in Ma	t$_c$ in Ma	(^{40}Ar/^{36}Ar)$_i$	SumS/(n-2) / n
0.88	0.0068	2.27 ± 0.41	12.4 ± 2.3	†	8.72	323.73	0.039					
2.00	0.0407	4.14 ± 0.05	22.6 ± 0.3	†	98.05	15136.48	0.024					
3.20	0.0576	4.30 ± 0.04	23.5 ± 0.2		96.13	7625.99	0.016					
4.50	0.0876	4.41 ± 0.05	24.1 ± 0.3	§	97.06	10052.72	0.014					
5.50	0.1415	4.43 ± 0.04	24.2 ± 0.2	§	98.69	22547.31	0.012					
6.50	0.0753	4.39 ± 0.04	24.0 ± 0.2	§	98.70	22721.53	0.013					
7.30	0.2813	4.45 ± 0.02	24.3 ± 0.1	§	95.67	6820.96	0.012					
7.50	0.1119	4.43 ± 0.02	24.2 ± 0.1	§	98.98	28989.58	0.012					
8.30	0.1974	4.46 ± 0.05	24.4 ± 0.3	§	98.01	14865.22	0.012	24.0 ± 0.2	24.2 ± 0.2	**24.1 ± 0.2**	322 ± 69	2.8 / 9

El Pajarito basalt 9-23-08-05 groundmass

pwr	F ^{39}Ar	^{40}Ar*/^{39}Ar$_K$	Age in Ma		% ^{40}Ar*	^{40}Ar/^{36}Ar^{37}Ar$_{Ca}$/^{39}Ar$_K$		t$_i$ in Ma	t$_p$ in Ma	t$_c$ in Ma	(^{40}Ar/^{36}Ar)$_i$	SumS/(n-2) / n
0.30	0.0064	46.0 ± 2.7	244.8 ± 13.2	†	70.50	1001.68	< 0.001					
0.70	0.0432	4.23 ± 1.07	24.0 ± 6.0	†	24.61	391.97	0.409					
1.20	0.1337	2.87 ± 0.15	16.3 ± 0.9		59.48	729.31	0.612					
1.80	0.2196	3.21 ± 0.06	18.2 ± 0.4	§	90.81	3215.28	0.656					
2.20	0.1687	3.36 ± 0.05	19.1 ± 0.3	§	80.00	1168.58	0.512					
2.80	0.1486	3.34 ± 0.05	18.9 ± 0.3	§	77.78	1030.68	0.433					
4.00	0.1552	3.19 ± 0.08	18.1 ± 0.4	§	94.22	5112.95	0.408					
7.00	0.1246	3.55 ± 0.07	20.1 ± 0.4	†	99.65	84031.11	0.809	20.2 ± 0.5	**18.6 ± 0.2**	18.8 ± 0.3	219 ± 19	0.8 / 5

pwr: laser power in watts applyied to release argon; age of the individual fraction does not include the uncertainty in J; t$_i$: integrated age; t$_p$: plateau age; t$_c$: isochron age calculated with all the fractions except those identified with the symbol †; (^{40}Ar/^{36}Ar)$_i$: initial (^{40}Ar/^{36}Ar) calculated from the inverse of the y-intercept of the isochron line in the correlation diagram (^{36}Ar/^{40}Ar) versus (^{39}Ar/^{40}Ar); SumS /(n-2) goodness of fit of the best straight line calculated and number of points used; § fractions selected for plateau calculation; ‡ isochron age calculated combining the fractions of the two experiments performed on the sample; all errors are given at 1σ level; J for El Toro Muerto basalt and Tetuachi ignimbrite samples is 0.003048 ± 0.000017; El Pajarito basalt sample was irradiated separately, J = 0.003157 ± 0.000050. t$_i$, t$_p$ and t$_c$ include the uncertainty in J. Preferred age is highlighted in bold typeface.

ben that developed during Late Oligocene–Early Miocene (Geological Society of America Time Scale, 2009) regional extension in the southern Basin and Range province. A maximum age for basin initiation is constrained to ~25 Ma (latest Oligocene) by contemporaneous bimodal volcanism of the El Toro Muerto basalt and the Tetuachi ignimbrite. The La Cieneguita member and El Toro Muerto basalt both floored the area prior to significant clastic deposition of the Arizpe conglomerate. The younger dated volcanic rocks in the Arizpe sub-basin is the Agua Caliente basalt (~21 Ma), which is interbedded in the upper part of the basin fill of the Báucarit Formation. These ages indicate that this was a rapidly subsiding basin as most of its sedimentary and volcanic accumulation occurred in a short period of time.

The Báucarit Formation is a 2.1 km-thick, east-dipping, clastic and volcanic succession whose tilting markedly decreases upsection from ~35º to 5-10º. The three fining-upward, multistoried pebble conglomerate sequences of the Arizpe conglomerate are interpreted to represent deposits of bed-load dominated streams in proximal braided rivers and/or mid alluvial fans. The sandstone and siltstone intervals in the upper parts of the middle and upper sequences indicate deposition in distal braidplains with associated development of lacustrine environments.

The factors controlling deposition of large-scale alluvial-fan sequences have been attributed to allocyclic forces such as tectonics and climate. We interpret that normal faulting that initiated subsidence of the downthrown block was the primary control on deposition of the fining-upward sequences in the Arizpe conglomerate, as well as relative uplift of the adjacent block to the east that fed detritus to the basin. This inference is based on the thickness of the succession, coarseness of the detritus, and unroofing of the source area as recorded by upward enrichment of volcanic clasts in the Arizpe conglomerate, derived from the Tarahumara Formation basement. The normal faulting that initiated the basin formation and subsequent basin development occurred close to the present eastern margin of this basin, as indicated by eastward tilting and internal growth strata geometry of the sedimentary fill. In this interpretation (following Einsele, 1992), active phases of normal faulting were responsible for deposition of each of the conglomerate sequences whereas the fine-grained intervals at their tops indicate periods of tectonic quiescence when retreat of the scarp front and lowering of relief of the source area occurred. Based on our geochronology, it

Table 4. Analitical data of U-Pb geochronological analyses for sample 11-20-07-2 from the El Picacho dome.

Analysis	U (ppm)	206Pb/204Pb	U/Th	Isotope ratios							Apparent ages (Ma)						Best age (Ma)	± (Ma)
				206Pb*/207Pb*	± (%)	207Pb*/235U*	± (%)	206Pb*/238U	± (%)	error corr.	206Pb*/238U	± (Ma)	207Pb*/235U	± (Ma)	206Pb*/207Pb*	± (Ma)		
1120072-3	185	438	0.7	15.8791	44.2	0.0327	44.6	0.0038	5.7	0.13	24.2	1.4	32.7	14.3	707.4	988.5	24.2	1.4
1120072-5	798	1746	0.6	20.2824	12.7	0.0259	12.8	0.0038	1.5	0.12	24.5	0.4	26.0	3.3	162.3	297.9	24.5	0.4
1120072-5A	232	636	0.8	16.8996	36.5	0.0298	36.9	0.0036	5.6	0.15	23.5	1.3	29.8	10.8	573.4	819.9	23.5	1.3
1120072-6	1374	3411	0.8	21.2384	9.7	0.0253	9.8	0.0039	1.0	0.10	25.0	0.2	25.3	2.4	53.5	232.0	25.0	0.2
1120072-9	219	612	0.5	15.2488	37.4	0.0353	38.0	0.0039	7.0	0.18	25.1	1.8	35.2	13.2	792.9	812.2	25.1	1.8
1120072-10	200	804	0.8	15.7289	37.1	0.0337	37.3	0.0038	3.8	0.10	24.8	0.9	33.7	12.4	727.6	813.7	24.8	0.9
1120072-11	180	549	0.6	25.2560	71.2	0.0193	72.6	0.0035	13.9	0.19	22.8	3.2	19.4	14.0	NA	NA	22.8	3.2
1120072-12	108	417	0.8	34.5985	102.0	0.0143	102.1	0.0036	5.7	0.06	23.1	1.3	14.4	14.6	NA	NA	23.1	1.3
1120072-13	94	426	0.7	14.2519	92.5	0.0353	93.1	0.0036	11.0	0.12	23.4	2.6	35.2	32.2	933.2	298.3	23.4	2.6
1120072-14	98	333	0.6	11.7129	152.4	0.0418	152.4	0.0035	4.0	0.03	22.8	0.9	41.6	62.1	1324.1	402.1	22.8	0.9
1120072-15	202	714	0.6	16.8684	57.2	0.0307	57.3	0.0038	3.5	0.06	24.2	0.9	30.7	17.4	577.5	1358.1	24.2	0.9
1120072-16	369	669	0.7	18.2514	31.3	0.0281	31.4	0.0037	1.8	0.06	23.9	0.4	28.1	8.7	403.7	717.8	23.9	0.4
1120072-17	327	615	0.9	14.5870	28.4	0.0334	29.1	0.0035	6.6	0.23	22.7	1.5	33.3	9.6	885.3	598.3	22.7	1.5
1120072-19	244	531	0.6	17.4180	36.1	0.0281	36.7	0.0035	6.2	0.17	22.8	1.4	28.1	10.2	507.4	819.5	22.8	1.4
1120072-20	480	582	0.6	15.6926	15.4	0.0336	15.5	0.0038	1.7	0.11	24.6	0.4	33.6	5.1	732.5	327.1	24.6	0.4
1120072-21	329	606	0.6	16.5240	24.6	0.0309	24.9	0.0037	3.5	0.14	23.9	0.8	30.9	7.6	622.1	539.0	23.9	0.8
1120072-22	302	435	0.5	15.6758	37.2	0.0348	37.4	0.0040	4.4	0.12	25.5	1.1	34.8	12.8	734.7	814.0	25.5	1.1
1120072-23	494	660	0.7	13.1005	29.1	0.0389	29.2	0.0037	1.0	0.03	23.8	0.2	38.7	11.1	1103.8	595.0	23.8	0.2
1120072-24	306	516	0.5	15.7717	23.0	0.0336	23.1	0.0038	2.2	0.10	24.7	0.5	33.6	7.6	721.8	493.7	24.7	0.5
1120072-25	222	327	0.6	9.8615	36.1	0.0499	36.2	0.0036	3.1	0.09	23.0	0.7	49.4	17.5	1650.0	692.8	23.0	0.7
1120072-26	135	657	0.7	16.7767	52.1	0.0297	52.6	0.0036	7.4	0.14	23.2	1.7	29.7	15.4	589.3	1211.7	23.2	1.7
1120072-27	83	438	0.8	14.0965	154.0	0.0363	154.2	0.0037	6.7	0.04	23.9	1.6	36.2	54.9	955.7	692.4	23.9	1.6
1120072-28	222	2298	2.0	16.1271	7.2	0.0863	7.3	0.0101	1.1	0.15	64.7	0.7	84.0	5.9	674.3	154.8	64.7	0.7
1120072-31	303	762	0.8	18.0251	20.4	0.0287	20.4	0.0037	1.2	0.06	24.1	0.3	28.7	5.8	431.5	459.1	24.1	0.3
1120072-32	466	948	0.5	17.1558	16.9	0.0291	17.1	0.0036	2.4	0.14	23.3	0.5	29.1	4.9	540.6	373.0	23.3	0.5
1120072-33	622	813	0.5	17.1981	10.4	0.0280	10.6	0.0035	2.2	0.20	22.4	0.5	28.0	2.9	535.2	227.8	22.4	0.5
1120072-34	118	636	0.6	17.4082	40.0	0.0274	40.8	0.0035	7.9	0.19	22.2	1.7	27.4	11.0	508.6	913.9	22.2	1.7

Mineral separation and U-Pb geochronology on individual zircon grains was conducted by laser-ablation-multicollector inductively coupled plasma-mass spectrometry (LA-MC-ICP-MS) at the Arizona LaserChron Center in the Department of Geosciences, University of Arizona using the procedures described by Gehrels *et al.* (2006). All age errors are quoted at 1σ (Ma) level, and errors for isotopic ratios are quoted at 1σ(%). NA= not available.
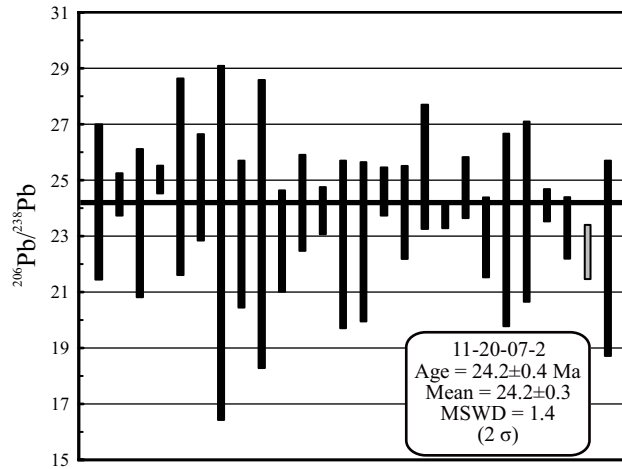
Figure 6. U-Pb histogram of age for sample 11-20-07-2 of the trachydacite from the Cerro El Picacho dome. The weight average age at 24.2 ± 0.4 Ma makes it of the same age as the El Toro Muerto basalt of the Báucarit Formation in the study area.

appears that initially the basin subsided relatively slow, between ~25 and 23.5 Ma when deposition of the La Cieneguita and El Toro Muerto basalt members occurred, and then subsidence rate became relatively faster by the time when the Arizpe conglomerate was being deposited (Figure 3b).

The most evident faults that crop out in the eastern margin of the basin are the El Fuste and the Granaditas faults (names according to González-Gallegos *et al.*, 2003, and traces modified in this work), which are parallel, planar normal faults that dip 80° to the west. Although these faults cut the younger stratigraphic member of the basin fill (El Catalán member), they could be older faults that were reactivated during the final stages of basin evolution. Otherwise, the main controlling fault(s) could be a less steeply-dipping fault that was covered beneath younger basin-fill, someplace west of the present basin margin. The uplifted block of the El Toro Muerto basalt that underlies the El Catalán breccia

Table 5. Data results of geochemical analyses of major, trace and REE for volcanic rocks of the study area.

Sample	6-3-05-1	2-15-07-1	10-9-06-1	6-3-05-3	11-20-07-2	9-23-08-5	4-8-08-3
Unit	EL Toro Muerto (lower part)	Toro Muerto (upper part)	Toro Muerto (upper part)	Agua Caliente basalt	El Picacho dome	El Pajarito basalt	El Huarache basalt
Age (Ma)	24.89 ± 0.64	23.5 ± 0.2	23.3 ± 0.3	21.29 ± 0.55	23.3 ± 0.6	18.6 ± 0.2	Not dated
Major oxides (wt. %)							
SiO_2	51.90	51.37	51.57	53.08	68.71	56.50	49.70
Al_2O_3	16.59	17.33	16.7	15.61	13.56	17.43	16.10
Fe_2O_3	9.78	8.66	9.74	8.52	1.32	6.48	10.60
MgO	4.24	3.51	4.06	2.79	0.27	2.39	3.61
CaO	6.96	6.63	7.02	7.26	1.11	5.80	9.00
Na_2O	4.01	3.89	3.95	3.60	3.57	3.98	3.61
K_2O	2.21	2.39	2.15	2.77	4.81	3.20	1.90
TiO_2	1.59	1.38	1.72	1.54	0.27	0.90	1.80
P_2O_5	0.649	0.60	0.63	0.71	0.05	0.50	0.60
MnO	0.15	0.13	0.19	0.11	0.05	0.08	0.14
LOI	1.80	3.70	2.00	3.70	1.35	2.00	1.80
TOT/C		0.01	<0.01	0.25			
TOT/S		<0.01	<0.01	<0.01			
SUM	99.96	99.59	99.75	99.7		99.5	99.7
A. I.		4.4	4.18	3.72	1.91		
Trace elements (ppm)							
Ba	1002	1012.	979.2	1123	984.0	1316	819
Be		2.0	2.0	2.0			
Co	27.0	27.6	29.7	25.2	22.0	18	37
Cs		2.3	0.7	2.1			
Ga		20.1	20.4	19.9			
Hf		7.0	6.7	8.6	9.4		
Nb	16.0	15.3	16.2	20.1	24.9	22	21
Rb	45.0	52.9	42.8	72.2	168.0	63	32
Sn		1.0	1.0	9.0			
Sr	710.0	713.8	769.1	624.5	127.0	698	649
Ta		0.7	0.8	0.9			
Th	<3.0	3.8	3.8	6.8	16.8	5	3

Continues →

Table 5 (continued). Data results of geochemical analyses of major, trace and REE for volcanic rocks of the study area.

Sample	6-3-05-1	2-15-07-1	10-9-06-1	6-3-05-3	11-20-07-2	9-23-08-5	4-8-08-3
U		1.2	1.0	1.8			
V	175	164	197	168	13.1	97	173
W		1.3	0.4	2.7			
Zr	241	303.1	277.2	378.1	261.0	374	227
Y	28	34.3	34.9	40.7	26.39	28	31
La	44.12	42.6	40.1	53.5	60.23	65.32	38.71
Ce	97.72	97.7	91.1	120.2	121.2	131.19	85.29
Pr	11.38	11.24	11.09	13.67	12.51	13.97	10.16
Nd	46.51	44.2	43.3	52.4	43.13	51.43	41.86
Sm	8.78	7.58	7.69	9.1	6.97	8.57	8.40
Eu	2.30	1.96	2.13	2.3	1.19	1.92	2.21
Gd	7.68	6.37	6.84	7.82	5.87	7.02	7.53
Tb	1.16	1.11	1.14	1.35	0.83	1.01	1.16
Dy	5.77	5	5.42	6.31	4.97	5.02	5.83
Ho	1.25	1.01	0.98	1.15	0.99	1.03	1.25
Er	3.24	2.8	2.77	3.26	2.98	2.82	3.27
Tm	0.44	0.43	0.45	0.54	0.44	0.41	0.44
Yb	2.91	2.59	2.72	3.04	3.12	2.74	2.89
Lu	0.45	0.4	0.41	0.45	0.46	0.41	0.45
Mo		0.5	0.4	0.9			
Cu	19	22.9	17.7	107.1	4	21	35
Pb	9	2.6	1.9	11.4	24.9	12	5
Zn	107	66	45	71	54	85	99
Ni	38	24.1	23.2	25.8	0		
As		5.2	5.7	13.4			
Cd		<0.1	0.1	0.2			
Sb		0.5	<0.1	0.3			
Bi		<0.1	<0.1	<0.1			
Ag		<0.1	<0.1	<0.1			
Au		<0.5	<0.5	<0.5			
Hg		0.21	0.01	0.01			
Tl		<0.1	0.1	<0.1			
Se		<0.5	<0.5	<0.5			
Cr	53				17	30	72
Cr$_2$O$_3$		0.003	0.007	0.007			
Ni	38.0	25.0	28.0	19.0	0.0	23	
Sc		14.0	16.0	14.0	0.0		

Samples 6-3-05-1, 9-23-08-5, and 4-8-08-3 were analyzed by XRF and ICP-MS in the Laboratorio Universitario de Geoquímica Isotópica, Universidad Nacional Autónoma de México. Samples 2-15-07-1, 10-9-06-1, and 6-3-05-3 were analyzed by XRF and ICP-MS at the Geosciences Department of the University of Arizona, and sample 11-20-07-2 was analyzed by HR-ICP-MS at the Department of Geology, University of Wisconsin-Eau Claire.

near the basin margin (Figure 2 section A-B) may indicate that synsedimentary tectonism was significant during basin evolution.

Other interpreted synsedimentary faults include the normal, NW-SE La Cieneguita and the Tetuachi faults (Figure 2). The former one affected the La Cieneguita member before deposition of the Toro Muerto basalt, while the latter one was active following deposition of the Tierras Prietas basalt and produced the horst that exposes the Tetuachi ignimbrite (Figure 2). On the other hand, the La Cieneguita and Tetuachi faults may be reactivated structures of a widespread, although still little documented NW-SE-striking normal faulting event that occurred in north-central

Sonora during Cenozoic time prior to Basin and Range tectonism (as reported by González-León *et al.*, 2000).

After deposition of the Báucarit Formation ceased, the Arizpe sub-basin was disorganized by a younger phase of normal faulting. The most important faults associated with this event are the NW-striking Crisanto and Tahuichopa faults, and probably the Las Higueritas fault (Figure 2). The Crisanto fault, in the southern part of the basin, uplifted the Tarahumara basement forming the NW-SE-oriented horst of Lomas El Quemado (Figure 2) and its downthrown block formed a basin to the southwest that was filled by the Sinoquipe conglomerate. The Sinoquipe conglomerate (informal name) is a poorly consolidated conglomerate
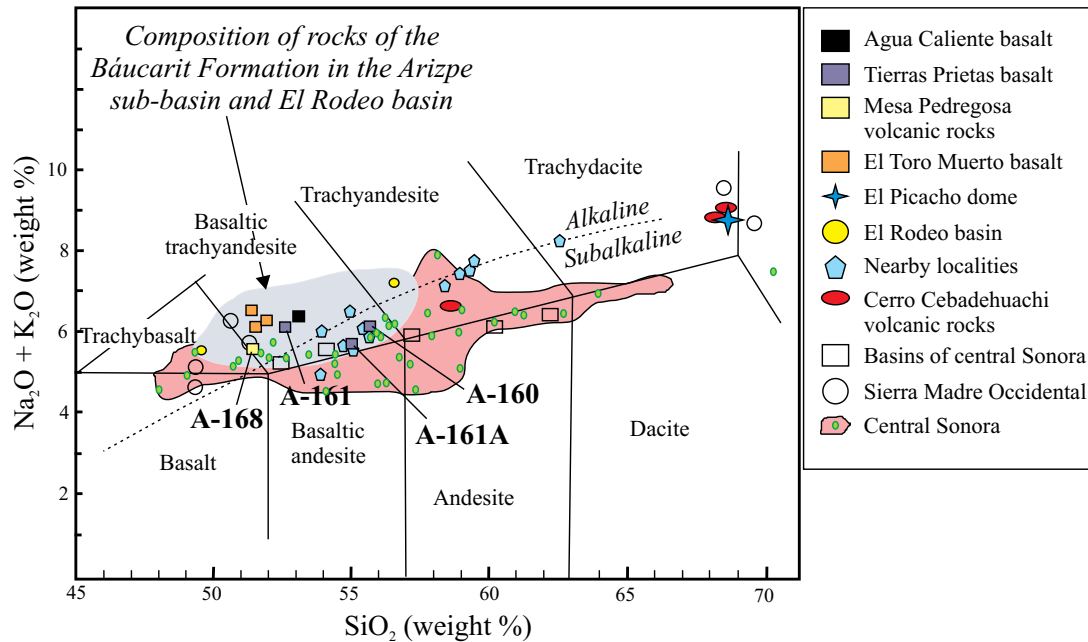
Figure 7. Total alkali *vs.* silica diagram (after LeBas *et al.*, 1986) of geochemical classification of volcanic rocks of the El Toro Muerto and Agua Caliente basalt members, including previous published data from the Tierras Prietas basalt (samples A-160, A-161 and A-161A from González-León *et al.*, 2000). Also plotted for comparison are data from the Mesa Pedregosa volcanic rocks (A-168 of González-León *et al.*, 2000) and our data from the El Huarache and El Pajarito basalts from the El Rodeo basins. Other data from volcanic rocks with ages between 28 to 17 Ma that are mentioned in the manuscript include: nearby areas of the Río Sonora region (blue pentagons) by Paz Moreno (1992); the Cerro Cebadéhuachi volcanic rocks (from González-León *et al.*, 2000), the Río Yaqui region (blank rectangles) (from McDowell *et al.*, 1997), western Sierra Madre Occidental (from Demant *et al.*, 1989) and data from central Sonora (Till *et al.*, 2009).

succession that we infer buries the Arizpe conglomerate in the Sinoquipe valley (Figure 2, section C-D). Evidence for this include the outliers of the El Toro Muerto basalt covered by this unit in the western margin of this sag, and the absence within it of the other basalt members of the Báucarit Formation that are present in the Arizpe sub-basin. The Tahuichopa fault deformed the Arizpe sub-basin in its northern part to form the Picacho de Arizpe horst, and its vertical displacement accounts for at least 2 km considering it exposes strata of the Bisbee Group and the Tarahumara Formation in this area (González-León *et al.*, 2000).

ARIZPE SUB-BASIN AND REGIONAL CONTEXT

The data herein reported from the Arizpe sub-basin help to constrain the time of extension and magmatism associated with the Basin and Range event in Sonora and in this section our results are compared with data reported from similar basins in other parts of the state.

Geochronology of magmatism herein reported form the Arizpe sub-basin most probably indicate an incomplete record of basin evolution constrained between ~25 and 21 Ma. The younger age of duration of the Basin and Range in this region of north-central Sonora, however, can be constrained by the age at near 18 Ma that we obtained from the El Pajarito basalt interbedded in the upper part of the

sedimentary fill of the El Rodeo basin (Figure 1). These data are consistent with the geochronology of volcanic rocks in basins of central and northern Sonora, which constrain basin initiation, between 27 to 25 Ma, to end at near 15 Ma. For instance, mafic rock of the Báucarit Formation in the Yécora basin were dated between ~24 and ~17 Ma (Cochemé and Demant, 1991), while at the Río Yaqui basin (Figure 1) the older volcanic rocks have ages between ~27 to 22 Ma and the younger are at ~17 Ma (McDowell *et al.*, 1997). Late Oligocene–Early Miocene ages were also obtained by Gans (1997) for basaltic rocks in the Santa Rosa area (Figure 1) and, for the Sahuaripa basin (Figure 1), Blair and Gans (2003) reported ages ~28 Ma for basaltic flows at the base of the Báucarit Formation, ~25 Ma for interbedded mafic flows, and ~15 Ma for andesitic flows in the upper part of the basin fill. In northern Sonora, the lower conglomerate of the Bacanuchi basin (González-León *et al.*, 2000) (Figure 1) interfingers with ~25 Ma rhyolitic tuffs of the "Mesa Pedregosa volcanic rocks" (González-León *et al.*, 2000) and both units unconformably overly the dacitic to rhyolitic succession of the "Cerro Cebadéhuachi volcanic rocks" dated between 28 and 27 Ma (González-León *et al.*, 2000). Basins associated to metamorphic core complexes such as the Magdalena, Tubutama and Ures basins (Figure 1) have interbedded mafic to rhyolitic volcanic rocks dated between ~27 and 15 Ma (Miranda-Gasca and DeJong, 1992; Miranda-Gasca *et al.*, 1998; Vega-Granillo and Calmus,
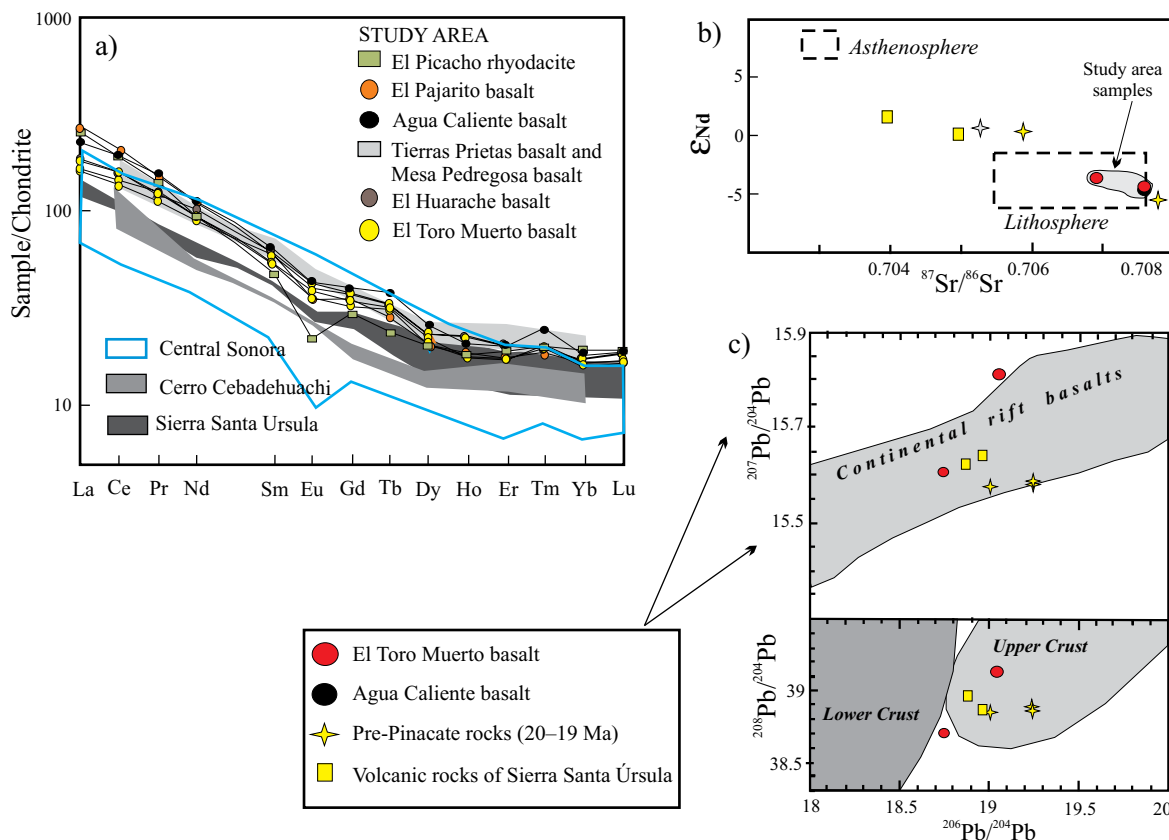
Figure 8. a) Rock RRE chondrite-normalized patterns for samples from the study area (including those from the El Huarache and El Pajarito basalts) compared with previous results from the Tierras Prietas basalt, and Mesa Pedregosa and Cerro Cebadéhuachi volcanic rocks from the Bacanuchi basin (González -León *et al.*, 2000). Comparison is also made with contemporaneous volcanic rocks of the Sierra Santa Úrsula (from Mora-Klepeis and McDowell, 2004) and central Sonora (Till *et al.*, 2009). b) εNd *vs.* ^{87}Sr/^{86}Sr diagram (after DePaolo and Daley, 2000) comparing our data with the pre-Pinacate suite of Vidal-Solano *et al.* (2008), and the La Espuela and Mezquite Formations from the Sierra Santa Úrsula (the εNd and the Sr initials values of these two formations were calculated from the Rb, Sr, Sm and Nd concentrations reported in tab. 1 of Mora-Klepeis and McDowell, 2004). c) ^{208}Pb/^{204}Pb *vs.* ^{206}Pb/^{204}Pb (after Zartman and Doe, 1981) and ^{207}Pb/^{204}Pb *vs.* ^{206}Pb/^{204}Pb (from Wilson, 2001) isotope correlation diagrams showing fields of upper and lower continental crust and continental rift basalts, respectively. Our data plotted along with contemporaneous pre-Pinacate rocks (Vidal-Solano *et al.*, 2008) and mafic rocks from Sierra Santa Úrsula (from Mora-Klepeis and McDowell, 2004) indicate apparent similar sources for these contemporaneous magmas.

2003; Wong and Gans, 2008).

Miocene magmatism along coastal Sonora with ages from ~23 and ~14 Ma is andesitic to rhyolitic, although its association to extensional basin development is not clearly documented. It occurs in the Sierra Santa Úrsula and in the San Carlos-Guaymas area (Mora-Álvarez and McDowell, 2000; Mora-Klepeis and McDowell, 2004) (Figure 1), in the Sierra Libre (MacMillan *et al.*, 2003) (Figure 1) and between Bahía de Kino and Puerto Libertad, including the Isla Tiburón (Gastil and Krummenacher, 1977; Gastil *et al.*, 1999) (Figure 1).

Most authors consider that the Sonoran Late Oligocene to Early Miocene magmatism was associated to extension that occurred in an intra-arc that developed during late stage subduction of the Farallon plate along the Pacific margin of northwest Mexico (*e.g.*, Demant *et al.*, 1989; Martin-Barajas, 2000; Gans, 1997; Umhoefer *et al.*, 2001; Mora-Klepeis and McDowell, 2004; Vidal-Solano *et al.*, 2008). Gans (1997) and Gans *et al.* (2007) also noted that major

extensional deformation migrated from eastern Sonora, where it occurred between 28 and 24 Ma, to coastal Sonora where it took place between 12 and 9 Ma.

The mafic rocks of the Báucarit Formation in the Arizpe sub-basin classify in a narrow range of alkaline basaltic trachyandesite, similar to contemporaneous flows of the nearby Mesa Pedregosa volcanic rocks (sample A-168 in Figure 7 taken from González-León *et al.*, 2000). Our samples from the El Rodeo basin and nearby areas reported by Paz-Moreno (1992) classify between trachybasalt and trachyandesite (Figure 7). Mafic flows in basins of the western Sierra Madre Occidental are alkaline trachybasalt and basaltic trachyandesite (Báucarit, Demant *et al.*, 1989; Cochemé and Demant, 1991) (Figure 7), and contemporaneous volcanic rocks of the Río Yaqui basin range from basaltic trachyandesite to andesite (McDowell *et al.*, 1997 (Figure 7). Similar rocks at the Bahía Kino–Puerto Libertad–Isla Tiburón region are mostly basalt and andesite (Gastil *et al.*, 1979). However, a more complete geochemical data

Table 6. Isotopic data from the El Toro Muerto and Agua Caliente basalt members of the Báucarit Formation in the study area.

Sample	6-3-05-3 Agua Caliente basalt	10-9-06-1 El Toro Muerto basalt (upper part)	2-15-07-1 El Toro Muerto basalt (upper part)
Rb	62.593	41.11	55.738
Sr	687.023	690.677	750.082
Rb/Sr	0.0911	0.0595	0.0743
$^{87}Rb/^{86}Sr$	0.261981	0.171143	0.213677
$^{87}Sr/^{86}Sr_{(t=0)}$	0.707594	0.706881	0.707575
std err %	0.0011	0.0012	0.0014
Sm	8.96	8.645	8.312
Nd	48.375	42.044	42.84
Sm/Nd	0.1852	0.2056	0.1941
$^{147}Sm/^{144}Nd$	0.111973	0.124699	0.117323
$^{143}Nd/^{144}Nd_{(t=0)}$	0.512388	0.512445	0.51239
std err%	0.0014	0.0012	0.0011
$\varepsilon Nd_{(t=0)}$	-4.88	-3.76	-4.84
Age (Ma)	21.3	24.9	23.5
$^{206}Pb/^{204}Pb$		18.7552	19.0294
$^{207}Pb/^{204}Pb$		15.6171	15.8241
$^{208}Pb/^{204}Pb$		38.6923	39.1189

Analysis were performed at the Isotopic Laboratory of the University of Arizona and methods are presented in the Appendix.

base of the mafic to intermediate volcanism from central Sonora with ages between ~28 and ~17 Ma, reported by Till *et al*. (2009), indicate a mostly subalkaline character with a compositional range from trachybasalt to andesite (Figure 7).

The REE chondrite-normalized patterns of our samples of the El Toro Muerto, Agua Caliente, El Huarache and El Pajarito basalts, and El Pichacho trachydacite (Figure 8a) plot in a narrow, consistent pattern along with the REE spectra obtained previously from the Tierras Prietas basalt and from the Mesa Pedregosa volcanic rocks (González-León *et al*., 2000) (Figure 8a). This pattern exhibit an enrichment in light REE and depletion in heavy REE; it is also similar but more differentiated than the REE spectra from the Cerro Cebadéhuachi volcanic rocks (Figure 8a), whose pattern resembles volcanic rocks (La Espuela and Mezquite formations) of the Sierra Santa Úrsula (Mora-Klepeis and McDowell, 2004) (Figure 8a). Our REE spectra are also similar to those of volcanic rocks from central Sonora with ages older than 14 Ma reported by Till *et al*. (2009).

Available regional isotopic data of nearly contemporaneous rocks are scarce and they are restricted to the Isla Tiburón, Sierra Santa Úrsula and El Pinacate areas. For the Isla Tiburón, Gastil *et al*. (1999) interpreted that Sr initial isotopic ratios varying between 0.7031 to 0.7055 in 20 to 15 M.y. old andesitic to dacitic rocks were compatible with a contaminated source in the mantle-wedge, without significant continental crust interaction. The Sr ratios reported by Mora-Klepeis and McDowell (2004) for the Sierra Santa Úrsula are low ($^{87}Sr/^{86}Sr$ = 0.7039) for the older andesitic

rocks (22 to 18 Ma), and more radiogenic for the younger dacitic rocks (18 to 15 Ma; $^{87}Sr/^{86}Sr$ = 0.7051 to 0.7055). The basalts from the study area have higher Sr initial ratios than the contemporaneous Isla Tiburón, Sierra Santa Úrsula, and the pre-Pinacate mafic rocks (20 to 19 Ma, Vidal-Solano *et al*., 2008), and when coupled with their negative εNd values they indicate that magmas were derived from partial melting of the attenuated continental lithosphere (Figure 8b). The Pb isotopic values of the El Toro Muerto basalt compare also with values of volcanic rocks of the sierra Santa Úrsula and the pre-Pinacate volcanics, and have signatures of continental rift basalts that form in the continental lithosphere (Figure 8c). In summary, the geochronology and geochemical data from the Arizpe sub-basin correlate well with interpretations on initiation, duration and magma composition of the Basin and Range regional setting, although no other basin in Sonora has been studied in detail regarding its sedimentary and volcanic fill.

CONCLUSIONS

The Arizpe sub-basin is a typical Basin and Range half-graben whose sedimentary and volcanic, east-dipping basin fill is the 2.1 km-thick Báucarit Formation that we divide into seven members. Basin duration is constrained between ~25 and ~21 Ma according to geochronology of the El Toro Muerto and Agua Caliente basalt members of its lower and upper parts, respectively. However, mafic flows interbedded in the upper part of the El Rodeo basin located just east of the study area may constrain age of duration of the Basin and Range event between ~25 and ~18 Ma in this region.

Normal faulting was probably the main controlling factor of basin subsidence and sedimentation. Subsidence was relatively slow between ~25 and 23.5 Ma during deposition of the La Cieneguita and El Toro Muerto basalt members, and then became relatively faster by the time the Arizpe conglomerate was being deposited. Faults that initiated basin formation are probably reactivated along the El Fuste and Granaditas faults, or they are buried beneath the younger fill of the basin. Synsedimentary and post-basin faults that disorganized the basin are NW-SE-, and N-S-striking normal faults.

Geochemical data indicate that magma composition of the older volcanic rocks in the basin is mafic and felsic. The El Toro Muerto, Tierras Priestas and Agua Caliente basalt members are mostly alkaline basaltic trachyandesite, and the ~23 Ma old, the El Picacho dome is trachydacite. This dome was the probably source of the Tetuachi ignimbrite. REE chondrite-normalized patterns of these rocks plot in a narrow, consistent pattern that exhibit enrichment in light REE and depletion in heavy REE which is consistent with contemporaneous magmatism of nearby basins. This pattern is also similar to the REE spectra of subalkaline volcanic rocks, basalt to dacite, with ages between 28 and 14 Ma

reported by Till *et al*. (2009) from central Sonora.

Our geochemical data coupled with isotopic analyses of the El Toro Muerto and Agua Caliente basalt members most probably indicate that magmatism of the Arizpe sub-basin corresponds to continental rift basalts derived from partial melting at the base of the continental lithosphere.

APPENDIX. ANALYTICAL METHODS

Ar-Ar dating

The $^{40}Ar/^{39}Ar$ analyses were performed at the Geochronology Laboratory of the Departmento de Geología, CICESE. The argon isotope experiments were conducted on rock fragments and sanidine crystals. These were heated with a Coherent Ar-ion Innova 70c laser. The extraction system is on line with a VG5400 mass spectrometer. All the samples and irradiation monitors, were irradiated in the U-enriched research reactor of University of McMaster in Hamilton, Canada, at position 5C in capsule CIC-55A and received a dose of 30 MW. To block thermal neutrons, the capsule was covered with a cadmium liner during irradiation. As irradiation monitors, aliquots of standard sanidine TCR-2 (split G93) (27.87 ± 0.04 Ma) and sanidine FCT-2C (27.84 ± 0.04 Ma) were irradiated alongside the samples and distributed among them to determine the neutron flux variations. Upon irradiation, the monitors were fused in one step while the samples were step-heated. The argon isotopes were corrected for blank, mass discrimination, radioactive decay of ^{37}Ar and ^{39}Ar and atmospheric contamination. For the Ca neutron interference reactions, the factors given by Masliwec (1984) were used. The decay constants recommended by Steiger and Jäger (1977) were applied in the data processing. The equations reported by York *et al*. (2004) were used in all the straight line fitting routines of the argon data reduction. The plateau age was calculated from the weighted mean of consecutive fractions that were in agreement within 1 σ. The error in the plateau, integrated and isochron ages includes the scatter in the irradiation monitors [J = 0.003048 ± 0.000017]. The analytical precision is reported as one standard deviation (1 σ). For each sample, the relevant $^{40}Ar/^{39}Ar$ data for all the experiments is presented, it includes the results for individual steps and the integrated ages. In the results table, the fractions selected to calculate the plateau age are identified as well as the fractions ignored in the isochron age calculation. The preferred age for each sample is highlighted in bold typeface.

Isotopic analysis

The isotopic ratios of $^{87}Sr/^{86}Sr$, $^{143}Nd/^{144}Nd$, and the trace element concentrations of Rb, Sr, Sm, and Nd were measured by thermal ionization mass spectrometry on whole rock samples. Rock samples were crushed to about one third of their grain size. Rock powders were put in large Savillex vials and dissolved in mixtures of hot concentrated $HF-HNO_3$ or alternatively, mixtures of cold concentrated $HF-HClO_4$. The dissolved samples were spiked with the Caltech Rb, Sr, and mixed Sm-Nd spikes (Wasserburg *et al*., 1981; Ducea and Saleeby, 1998) after dissolution. Rb, Sr, and the bulk of the REEs were separated in cation columns containing AG50W-X4 resin, using 1N to 4N HCl. Separation of Sm and Nd was achieved in anion column containing LN Spec resin, using 0.1N to 2.5N HCl. Rb was loaded onto single Re filaments using silica gel and H_3PO_4. Sr was loaded onto single Ta filaments with Ta_2O_5 powder. Sm and Nd were loaded onto single Re filaments using platinized carbon, and resin beads, respectively.

Mass spectrometric analyses were carried out at the University of Arizona on an automated VG Sector multi-collector instrument fitted with adjustable 10^{11} Ω Faraday collectors and a Daly photomultiplier (Ducea and Saleeby, 1998). Concentrations of Rb, Sr, Sm, Nd were determined by isotope dilution, with isotopic compositions determined on the same spiked runs. An off-line manipulation program was used for isotope dilution calculations. Typical runs consisted of acquisition of 100 isotopic ratios. The mean result of ten analyses of the standard NRbAAA performed during the course of this study is: $^{85}Rb/^{87}Rb = 2.61199\pm20$. Fifteen analyses of standard Sr987 yielded mean ratios of: $^{87}Sr/^{86}Sr = 0.710285\pm7$ and $^{84}Sr/^{86}Sr = 0.056316\pm12$. The mean results of five analyses of the standard nSmβ performed during the course of this study are: $^{148}Sm/^{147}Sm = 0.74880\pm21$, and $^{148}Sm/^{152}Sm = 0.42110\pm6$. Fifteen measurements of the LaJolla Nd standard were performed during the course of this study. The standard runs yielded the following isotopic ratios: $^{142}Nd/^{144}Nd = 1.14184\pm2$, $^{143}Nd/^{144}Nd = 511853\pm2$, $^{145}Nd/^{144}Nd = 0.348390\pm2$, and $^{150}Nd/^{144}Nd = 0.23638\pm2$. The Sr isotopic ratios of standards and samples were normalized to $^{86}Sr/^{88}Sr = 0.1194$, whereas the Nd isotopic ratios were normalized to $^{146}Nd/^{144}Nd = 0.7219$. The

estimated analytical ±2σ uncertainties for samples analyzed in this study are: $^{87}Rb/^{86}Sr = 0.35\%$, $^{87}Sr/^{86}Sr = 0.0014\%$, $^{147}Sm/^{144}Nd = 0.4\%$, and $^{143}Nd/^{144}Nd = 0.0012\%$. Procedural blanks averaged from five determinations were: Rb 10 pg, Sr 150 pg, Sm 2.7 pg, and Nd 5.5 pg.

Washes from the cation column separation were used for separating Pb in Sr-Spec resin (Eichrom, Darien, IL) columns by using protocol developed at the University of Arizona. Samples were loaded in 8M HNO_3 in the Sr spec columns. Pb elution is achieved via 8M HCl. Lead isotope analysis was conducted on a GV Instruments (Hudson, NH) multicollector inductively coupled plasma mass spectrometer (MC-ICPMS) at the University of Arizona (Thibodeau *et al.*, 2007). Samples were introduced into the instrument by free aspiration with a low-flow concentric nebulizer into a watercooled chamber. A blank, consisting of 2% HNO_3, was run before each sample. Before analysis, all samples were spiked with a Tl solution to achieve a Pb/Tl ratio of 10. Throughout the experiment, the standard National Bureau of Standards (NBS)-981 was run to monitor the stability of the instrument.

All results were Hg-corrected and empirically normalized to Tl by using an exponential law correction. To correct for machine and interlaboratory bias, all results were normalized to values reported by Galer and Abouchami (2004) for the National Bureau of Standards NBS-981 standard ($^{206}Pb/^{204}Pb = 16.9405$, $^{207}Pb/^{204}Pb = 15.4963$, and $^{208}Pb/^{204}Pb = 36.7219$). Internal error reflects the reproducibility of the measurements on individual samples, whereas external errors are derived from longterm reproducibility of NBS-981 Pb standard and result in part from the mass bias effects within the instrument. In all cases, external error exceeds the internal errors and is reported below. External errors associated with each Pb isotopic ratio are as follows: $^{206}Pb/^{204}Pb = 0.028\%$, $^{207}Pb/^{204}Pb = 0.028\%$, and $^{208}Pb/^{204}Pb = 0.031\%$.

REFERENCES

Blair, K., Gans, P.B., 2003, Stratigraphy of the Sahuaripa basin and preliminary comparison to the Río Yaqui basin, east-central Sonora, Mexico: Geological Society of America Abstracts with Programs, 34(6), 16-13

Calles-Montijo, R.., 1999, Evolucion tectonosedimentaria de las cuencas terciarias: Porción sur cuenca de Ures y Punta de Agua, Sonora Central, Mexico: Universidad de Sonora, tesis de maestría, 67 pp.

Cochemé, J.J., Demant, A., 1991, Geology of the Yécora area, northern Sierra Madre Occidnetal, Mexico in Pérez-Segura, E., Jacques-Ayala, C. (eds.), Studies of Sonoran geology: Boulder, Colorado, Geological Society of America, Special Paper 254, 81-94.

De la O-Villanueva, M., 1993, Sedimentología y petrografía de la Formación Báucarit (Mioceno) en la cuenca de Tonichi-La Dura, Sonora, México: Universidad Autónoma de Nuevo León, Facultad de Ciencias de la Tierra, Tesis de Maestría, 88 pp.

Demant, A., Cochemé, J.J., Delpretti, P., Piguet, P., 1989, Geology and petrology of the Tertiary volcanics of the northwestern Sierra Madre Occidental, Mexico: Bulletin Societé Géologique France, 8, 737-748.

DePaolo, D.J., Daley, E.E., 2000, Neodymium isotopes in basalts of the southwest basin and range and lithospheric thinning during continental extension: Chemical Geology, 169(1), 157-185.

Ducea, M.N., Saleeby, J.B., 1998, The age and origin of a thick mafic ultramafic root from beneath the Sierra Nevada batholiths: Contributions to Mineralogy and Petrology, 133(1-2), 169-185.

Einsele, G., 1992, Sedimentary basins, evolution, facies and sediment budget: Germany, Springer-Verlag, 628 pp.

Galer, S.J.G., Abouchami, W., 2004, Mass bias correction laws suitable for MC-ICP-MS measurement (abstract), in 14th Annual Goldschmidt conference,: Geochimica et. Cosmochimica Acta, 68, A542.

Gans, P.B., 1997, Large-magnitude Oligo-Miocene extension in southern Sonora: implications for the tectonic evolution of northwest Mexico: Tectonics, 16(3), 388-408.

Gans, P., Wong, M., Blair, K., Macmillan, I., Roldán, J., Till, C., Herman, S., 2007, Cenozoic structural and magmatic evolution of Sonora: the transition from intra-arc extension to trans-tensional rifting: Ores and Orogenesis, A symposium honoring the career of William R. Dickinson: Tucson, Arizona, Geological Society of America, Program with Abstracts, 97-98.

Gastil, R.G., Krummenacher, D., 1977, Reconnaissance geology of coastal Sonora between Puerto Lobos and Bahia Kino: Geological Society of America Bulletin, 88(2), 189-198.

Gastil, R.G., Krummenacher, D., Minch, J., 1979, The record of Cenozoic volcanism around the Gulf of California: Geological Society of America Bulletin, 90(9), 839-857.

Gastil, R.G., Neuhaus, J., Cassidy, M., Smith, J.T., Ingle, J.C., Krummenacher, D., 1999, Geology and paleontology of southwestern Isla Tiburón, Sonora, Mexico: Revista Mexicana de Ciencias Geológicas, 16(1), 1-34.

Gehrels, G., Valencia, V., Pullen, A., 2006, Detrital Zircon Geochronology by Laser Ablation Multicollector ICPMS at the Arizona LaserChron Center, in Olszewski, T.D. (ed.), Geochronology: Emerging Opportunities: Paleontology Society Papers, 12, 67-76.

Geological Society of America, 2009, Geologic Time Scale: <http://www.geosociety.org/science/timescale/>.

González-Gallegos, A., Morales Morales, H., Orantes Contreras, V., 2003, Carta Geológico-Minera Arizpe H12B73, Sonora, escala 1:50,000: Consejo de Recursos Minerales, Gobierno Federal.

González-León, C., McIntosh, W.C., Lozano-Santacruz, R., Valencia-Moreno, M., Amaya-Martínez, R., Rodríguez Castañeda, J.L., 2000, Cretaceous and Tertiary sedimentary, magmatic, and tectonics evolution of north-central Sonora (Arizpe and Bacanuchi quadrangles), northwest Mexico: Geological Society of America Bulletin, 112(4), 600-611.

King, R.E., 1939, Geological reconnaissance in northern Sierra Madre Occidental of Mexico: Geological Society of America Bulletin, 50(11), 1625-1722.

Le Bas, M.J., Le Maitre, R.W., Streckeisen, A., Zanetti, B., 1986, A Chemicals classification of volcanic rocks based on the total alkali-silica diagram: Journal of Petrology, 27(3), 745-750.

MacMillan, I., Gans, P., Roldán, J., 2003, Mid-Miocene silicic volcanism and rapid extension in the Sierra Libre, Sonora, Mexico (abstract): Geological Society of America, Abstract with Programs, 35(4), p. 26.

Mahood, G., Drake, R.E., 1982, K-Ar dating young rhyolitic rocks: a case study of the Sierra La Primavera, Jallisco, Mexico: Geological Society of America Bulletin, 93(12), 1232-1241.

Martin Barajas, A., 2000, Volcanismo y extension en la Provincia Extensional del Golfo de California: Boletín de la Sociedad Geológica Mexicana, 53, 72-83.

Masliwec A., 1984, Applicability of the $^{40}Ar/^{39}Ar$ method to the dating of ore bodies: University of Toronto, Ph. D. Thesis.

McDowell, F.W., Roldán-Quintana, J., Amaya-Martínez, R., 1997, Interrelationship of sedimenary and volcanic deposits associated with Tertiary extension in Sonora, Mexico: Geological Society of America Bulletin, 109(10), 1349-1360.

Miranda-Gasca, M., DeJong, K.A., 1992, The Magdalena mid-Tertiary extensional basin, in Clark, K.F., Roldán-Quintana, J., Schmidt, R.H.(eds.), Geology and Mineral Resources of Northern Sierra

Madre Occidental, Mexico: El Paso Geological Society, Field Conference, Guidebook, 377-384.

Miranda-Gasca, M., Gomez-Caballero, J.A., Eastoe, C.J., 1998, Borate deposits of northern Sonora, Mexico: stratigraphy, tectonics, stable isotopes, and fluid inclusions: Economic Geology, 93(4), 510-523.

Mora-Alvarez, G., McDowell, F.W., 2000, Miocene volcanism during late subduction and early rifting in the Sierra Santa Ursula of western Sonora, Mexico, *in* Delgado-Granados, H., Aguirre-Díaz, G., Stock, J.M. (eds.), Cenozoic tectonics and volcanism of Mexico: Geological Society of America, Special Paper 334, 123-141.

Mora-Klepeis, G., McDowell, F.W., 2004, Late Miocene calc-alkalic volcanism in northwestern Mexico: an expression of rift or subduction-related magmatism?: Journal of South American Earth Sciences, 17(4), 297-310.

Paz Moreno, F.A., 1992, Le volcanisme Mio-Plio-Quaternaire de l'etat du Sonora (nord-ouest du Mexique): evolution spatiale et chronologique; implications petrogenetiques: Université de Droit, d'Economie et des Sciences d'Aix-Marseille, these Docteur en Sciences, 250 pp.

Steiger, R.H., Jäger, E., 1977, Subcommission on Geochronology: Convention on the use of decay constants in Geo and Cosmochronology: Earth and Planetary Sciences Letters, 36(3), 359-362.

Thibodeau, A.M., Killick, D.J., Ruiz, J., Chesley, J.T., Deagan, K., Cruxent, J.M., Lyman, W., 2007, The strange case of the earliest silver extraction by European colonists in the New World: Proceedings of the National Academy of Sciences of the United States of America, 104(9), 3663-3666.

Till, C.B., Gans, P.B., Spera, F.J., MacMillan, I., Blair, K.D., 2009, Perils of petrotectonic modeling: A view from southern Sonora, Mexico: Journal of. Volcanology and Geothermal. Research, 186(3-4), 160-168.

Umhoefer, P.J., Dorsey, R.J., Willsey, S., Mayer, L., Renne, P., 2001, Stratigraphy and geochronology of the Comondú Group near Loreto, Baja California sur, Mexico: Sedimentary Geology, 144(1-2), 125-147.

Vega-Granillo, R., Calmus, T., 2003, Mazatan metamorphic core complex (Sonora, Mexico): structures along the detachment fault and its exhumation evolution: Journal of South American Earth Sciences, 16(4), 193-204.

Vidal-Solano, J.R., Demant, A., Paz Moreno, F.A., Lapierre, H., Ortega-Rivera, M.A., Lee, J.K:W., 2008, Insights into the tectonomagmatic evolution of NW Mexico: Geochronology and geochemistry of the Miocene volcanic rocks from the Pinacate area, Sonora: Geological Society of America Bulletin, 120(5-6), 691-708.

Wasserburg , G.J., Jacobsen, S.B., DePaolo, DJ., McCulloch, M.T., Wen, T., 1981, Precise determination of Sm/Nd ratios, Sm and Nd isotopic abundances in standard Solutions: Geochimica et Cosmochimica Acta, 45, 2311-2323.

Wilson, M., 2001, Igneous petrogenesis: The Netherlands, Kluger Academic Publishers, 466 pp.

Wong, M.S., Gans, P.B., 2008, Geologic, structural and thermochronological constraints on the tectonic evolution of the Sierra Mazatán core complex, Sonora, Mexico: New insighits into metamorphic core complex formation: Tectonics 27(TC4013), doi:10.1029/2007TC002173.

York, D., Evensen, N.M., López-Martínez, M., De Basabe-Delgado, J., 2004, Unified equations for the slope, intercept, and standard errors of the best straight line: American Journal of Physics, 73(3), 367-375.

Zartman, R.E, Doe, B.R.., 1981, Plumbotectonics-The model: Tectonophysics, 75(1-2), 135-162.